Supporting Information

Process-Intensified Enzymatic Decarboxylation using Immobilized Arylmalonate Decarboxylase for Sustainable Asymmetric Synthesis of α-Arylpropionic Acids

Jan Gerstenberger, [a] Timm Werbilo, [a] Marvin Haas, [a] Simona Serban, [b] Alessandra Basso, [b] Pablo Domínguez de María, [c] and Selin Kara*[a,d]

[a] J. Gerstenberger, T. Werbilo, M. Haas, Prof. Dr.-Ing. habil. S. Kara
Institute of Technical Chemistry
Leibniz University Hannover
Callinstraße 5, 30167 Hannover, Germany
E-mail: selin.kara@iftc.uni-hannover.de

[b] Dr. S. Serban, Dr. A. Basso
Sunresin New Materials
Sunresin Park, Xi'an Hi-tech Industrial Development Zone Xian, Shaanxi, P. R. China

[c] Dr. habil. Pablo Domínguez de María
Sustainable Momentum SL,
35011 Las Palmas de Gran Canaria, Canary Islands, Spain

[d] Prof. Dr.-Ing. habil. S. Kara
Biocatalysis and Bioprocessing Group, Department of Biological and Chemical Engineering
Aarhus University
Gustav Wieds Vej 10, 8000 Aarhus C, Denmark
E-mail: selin.kara@bce.au.dk

1 General Information

1.1 Atom economy

The atom economy was calculated by **equation (S1)**, with the molecular weight of the respective base used in the saponification procedure. In the case of the hydrogenolysis, two equivalents of hydrogen were accounted for. The calculated atom economy is summarized in **Table S1**.

$$atom\ economy = \frac{molecular\ weight\ of\ desired\ product}{molecular\ weight\ of\ all\ reactants} \cdot 100\% \quad \text{(S1)}$$

Table S1. Atom economy of the benzylic ester (Bn) protection strategy compared to the utilized methyl ester (Me) protection strategy integrated in our process. The atom economy was calculated by equation (S1) based on two equivalents of H_2 for the benzylic ester deprotection and two equivalents of base used for deprotection according to the saponification procedures described in **Section 4**; NaOH was utilized for **1c**, **2c**, **4c,** and **5c**, LiOH was utilized for **3c**.

Product	**Atom economy [%]**	
	Bn-protection	Me-protection
Naproxen (1c)	59.8	72.7
Flurbiprofen (2c)	60.5	71.7
2-phenylpropionic acid (3c)	51.0	71.9
2-methylbut-3-enoic acid (4c)	30.5	39.7
2-ethylbut-3-enoic acid (5c)	33.3	42.9

1.2 Chemicals

All commercially available chemicals and solvents were purchased from Acros Organics, Thermo Fisher Scientific, Carl-Roth, Sigma-Aldrich, TCI, VWR, and used without further purification, unless otherwise stated.

1.3 Escherichia coli strains

Recombinant *Bb*AMDase IPLL and *Bb*AMDase ICPLLG were expressed in *E. coli* BL21 (DE3) (genotype: F- ompT hsdSB ($r_B^- m_B^-$) gal dcm (DE3)). The corresponding plasmids were provided by the research group of Prof. Robert Kourist (Institute of Molecular Biotechnology, Graz University of Technology) and are thankfully acknowledged.

1.4 Transformation of competent *E. coli* cells

Transformation of competent in *E. coli* BL21 (DE3) was carried out by thawing an aliquot of competent cells (50 µL) on ice and addition of 2 µL of plasmid DNA to the cell suspension. The mixture was incubated on ice for 30 min. A heat-shock at 42 °C was applied for 30 seconds utilizing a water bath. LB-SOC medium (400 µL) was added, and the mixture was incubated at 37 °C (250 rpm,1 h). 50 µL of the incubated cell mixture was spread on LB agar plates (30 µg/mL kanamycin) and incubated at 37 °C overnight.

1.5 Overnight cultures

Overnight cultures (ONC) of *E. coli* BL21 (DE3) for the production of AMDase (wildtype-*Bb*, IPLL, ICPLLG) were inoculated by the addition of 20 µL glycerol stock (or selected colony after transformation) to 15 mL lysogeny broth (LB)-media (Kanamycin 40 µg/mL). The ONC's were incubated overnight at 37 °C (120 rpm, 16 h) and directly used for the main cultivations.

1.6 Glycerol stocks

Cultures were maintained in 25% (v/v) glycerol stocks at -80 °C. For this purpose, 50% (v/v) sterile glycerol was mixed with the respective overnight culture in a 1:1 ratio in cryogenic tubes. The prepared glycerol stocks were incubated on ice for 20 min and were subsequently frozen. The glycerol stocks were replaced after repeated use.

1.7 Cultivation of *E. coli* for AMDase production

The enzyme utilized in the preparative scale reaction was produced according to a high cell density (HCD) cultivation recently developed in our laboratories.[28] All other AMDase strains (wildtype-*Bb*, IPLL and ICPLLG) utilized in this study were produced utilizing shake flasks with 1 L LB-media for *E. coli* BL21 (DE3) cultivation.

The shake flask cultivations were carried out by adding the entire preculture for inoculation (37 °C, 70 rpm, OD_{600} of ~0.08) of the main culture (1 L LB-media, 30 µg/mL Kanamycin). Protein production was induced with IPTG (1 mM, OD_{600} of 0.9) and the culture was incubated further (22 h, 28 °C, 70 rpm). The cells were harvested via centrifugation (4000 rpm, 4 °C, 25 min). The cell pellet was washed twice with TRIS-HCl buffer (50 mL, 50 mM, pH 8, 4 °C) and subsequently shock frozen in liquid nitrogen, to be stored at -20 °C until usage.

1.8 Buffer compositions

Composition of buffers and media utilized in this study are listed in **Table S2**–**Table S4**. For the determination of specific activity, phenylmalonic acid (20 mM) was utilized as model substrate and dissolved the respective buffer, with subsequent pH adjustment as indicated in the respective experimental section.

Table S2. Overview of 1000-fold stock solution used for *E. coli* cultivation for the production of AMDase. Kanamycin antibiotics stock solution (40 mg/mL) and Isopropyl-β-D-thiogalactopyranoside (IPTG) stock solution (1 M) for gene expression were 0.22 µM filtered and stored at -20 °C until usage.

Stock solution	Reagent	Amount
Kanamycin stock (40 mg/mL)	Kanamycin	400 mg
	ddH_2O	10 mL
IPTG stock (1 M)	IPTG	2.3818 g
	ddH_2O	10 mL

Table S3. Overview of utilized reaction buffers. The buffers were stored at 4 °C until usage.

Buffer	Reagent	Amount	Concentration [mM]
TRIS-HCl buffer	TRIS	6.06 g	50
	HCl (37%)	2.3 mL	
	adjust to pH 8		
	ddH_2O	*ad* 1000 mL	
HEPES buffer	HEPES	11.92 g	50
	adjust to pH[a]		
	ddH_2O	*ad* 1000 mL	
MES buffer	$MES{\cdot}H_2O$	2.67 g	50
	adjust to pH[a]		
	ddH_2O	*ad* 250 mL	
MOPS buffer	MOPS	2.62	50
	adjust to pH[a]		
	ddH_2O	*ad* 250 mL	
AMPSO buffer	AMPSO	2.84	50
	adjust to pH[a]		
	ddH_2O	*ad* 250 mL	
KPi (pH 7.9)	K_2HPO_4	1.95	44.7
	KH_2PO_4	0.18	5.3
	ddH_2O	*ad* 250 mL	

[a] The pH was adjusted manually to the value indicated in the respective experimental procedure.

Table S4. Overview of utilized immobilization buffers. The buffers were stored at 4 °C until usage.

Buffer	Reagent	Amount	Concentration [mM]
Covalent immobilization buffer	HEPES	11.9 g	50
	NaCl stock (5M)	10 mL	50
	adjust pH to 6.8		
	ddH_2O	*ad* 1000 mL	
Covalent washing buffer	HEPES	6.0 g	50
	NaCl stock (5M)	50 mL	500
	adjust pH to 6.8		
	ddH_2O	*ad* 500 mL	
Affinity immobilization buffer	HEPES	11.9 g	50
	Imidazole	680.8 mg	10
	NaCl stock (5M)	10 mL	50
	adjust pH to 7.4		
	ddH_2O	*ad* 1000 mL	
Affinity washing buffer	HEPES	6.0 g	50
	Imidazole	680.8 mg	10
	NaCl stock (5M)	50 mL	500
	adjust pH to 7.4		
	ddH_2O	*ad* 500 mL	

1.9 Bayesian Optimization

Bayesian Optimization (BO) of two parameters (pH and temperature) of the RBR was carried out by the incorporation of two response values (*ee* and specific activity) in a MATLAB script written by JG and TW. The main logic is based on MATLAB's '*bayesopt'* function. This proved to be a robust approach, as the main loop is internally constructing the Gaussian Process[65] (GP) surrogate model and kernel selection to suggest the next experimental point. We decided to implement only a few tunable parameters in the script, as compromise between complexity and accuracy. The parameters '*weights.ee*' and '*weights.activity*' allow for the adjusted optimization of the responses according to their value of desirability w_i given by the user. The overall desirability OD is represented as '*scalar_obj*' in the script, is calculated by **equation** (**S2**) where *k* is the number of responses.[66,67]

$$OD = \left(\prod_{i=1}^{k} d_i^{w_i} \right)^{\frac{1}{\sum_{i=1}^{k} w_i}} \tag{S2}$$

The individual desirability scores d_i for enantiomeric excess and specific activity are calculated by the script with their respective GP function and normalized to a range between 0 and 1 before being weighted by their respective desirability w_i. For this specific use-case, the desirability for the enantiomeric excess is normalized against the theoretical upper limit of 100%. The desirability for the specific activity utilizes a dynamic max-scaling approach, normalizing against the highest experimental value observed within the current dataset. This allows direct utilization of the BO-script on other use-cases with different activities.

To ensure a well-distributed initial search space and prevent the optimizer from converging prematurely on local optima, the script utilizes Latin Hypercube Sampling (LHS) for the primary data points, as a near-random approach. A '*lhs_buffer*' parameter is used to concentrate initial points within a smaller sub-section of the parameter range if the optimum's location is anticipated from prior data, while still permitting the optimizer to eventually explore the full experimental design space.

The '*explorationRatio'* directly influences the optimization logic by balancing the exploration of unknown regions against the exploitation of known optima. Given that laboratory experiments are subject to inherent practical inaccuracies, we implemented a mechanism to prevent the clustering of data points in early iterations. This is because the information gain from very similar experimental conditions is often obscured by the standard deviation of the measurements. Furthermore, the parameters '*threshold*' and '*edge_threshold*' prevent such clustering during specified iteration intervals by calculating normalized distance vectors to previous data points by interfering with the '*explorationRatio'* parameter. If a suggested point is too close to an existing one or a boundary, the script applies a repulsion force until it satisfies the minimum distance threshold. This approach reduces uncertainty across the entire parameter range in the early stages—reflecting the standard deviations of experimental data—at the cost of slower optimization on smooth, synthetic data.

The latest versions of the scripts can be downloaded at:
https://gitlab.uni-hannover.de/jan11jan/bayesian_optimization/-/releases/JG_BO_1.0.1

For a comprehensive guide on Bayesian optimization in bioprocess engineering the reader is advised to the referenced literature.[68]

1.9.1 Test mode option in the BO-MATLAB script

To ensure algorithmic robustness prior to laboratory deployment, we implemented a synthetic 'Test Mode' utilizing benchmark functions (Ackley, Rosenbrock, Rastrigin) with tunable noise and complexity. These functions were modified to include coordinate shifts to ensure the optima did not default to the origin. This *in silico* validation phase served to verify its convergence behaviour and test until failure. To quantify the algorithm's precision in locating the global optimum within the design space, we introduced the *Normalized Parameter Proximity* (*NPP*). This metric is derived from the normalized Euclidean distance (d_{norm}) in the range ($x_{\mathrm{min},i}$, $x_{\mathrm{max},i}$) of the design space between the query point (x_i) and the theoretical optimum (x_i^*) by **equation (S3)** and **(S4)**. Where D is the dimensionality (in this study, $D = 2$, for two factors) of the search space. A high NPP corresponds to good overlap of the synthetic optimum and the suggested optimum by the script.

$$d_{\mathrm{norm}}(x, x^*) = \sqrt{\sum_{i=1}^{D} \left(\frac{x_i - x_i^*}{x_{\mathrm{max},i} - x_{\mathrm{min},i}} \right)^2} \tag{S3}$$

$$NPP = 100 \cdot \left(1 - \frac{d_{\mathrm{norm}}}{\sqrt{D}} \right) \tag{S4}$$

1.9.2 Validation of the BO-MATLAB script

For all validation tests of the BO-MATLAB script the factor range was set to the values of the experimental study (pH: 5.5–9.7, temperature: 10–45) with a maximum of 20 iterations. The '*explorationRatio'* was set to the default value of 0.5, as exploration was controlled with the threshold parameters. The threshold parameters listed in **Table S5**, proved to be a solid compromise of exploration and exploitation. The high threshold values are accounting for usual standard deviation of manual experiments to determine experimental differences in most use cases. The edge threshold reflects the anticipation of the maximum and reduces the factor range to be screened. Thereby uncertainty is reduced in that factorial area, while the full factor range is considered in later iterations if necessary. As this option has high risk of user-bias, it is meant to be toggled off when no anticipation can be made.

Table S5. Threshold parameters utilized for the validation experiments on synthetic data.

Iteration	Threshold type	Value
<9	threshold	0.20
	edge_threshold	0.15
<14	threshold	0.12
	edge_threshold	0.08
>14	threshold	0.00
	edge_threshold	0.04

1.9.2.1 Different maximum settings of smooth hill-climbing Ackley functions

For the first test, the optimizer was set to find the balanced optimum of two overlapping smooth Ackley functions[69] with different location of the function's maximum. The applied function was calculated according to **equation (S5)**, where the modification $dx = x - x_t$ and $dy = y - y_t$ enables shifting of the optimum in the script settings. The utilized parameters of the functions are listed in **Table S6.** In **Table S7** the conditions are listed over the iterations along with the *NPP* values to the balanced optimum at pH 7.5 and 25 °C. Further, the calculated response surfaces of the different GP-models are shown along the uncertainty of the balanced model in **Figure S1**.

$$f(x,y)_{\text{Ackley}} = -a \cdot e^{\left(-b\sqrt{0.5((dx)^2+(dy)^2)}\right)} - e^{(0.5(\cos(c(dx)) + \cos(c(dy))))} + a + e \quad \text{(S5)}$$

Table S6. Parameter setting for the optimization of two overlapping smooth Ackley functions. Randomized noise was not applied.

***ee* function: Ackley, maximum at pH 7, 20 °C**	**Max. value = 100; *a* = 20, *b* = 0.2, *c* = 0**
Activity function: Ackley, maximum at pH 8, 30 °C	Max. value = 250; *a* = 20, *b* = 0.2, *c* = 0

Table S7. Experimental settings over 20 iterations and the predicted maximum of the current balanced GP model after the initial data points by LHS. Synthetic data was utilized according **Table S6**. The balanced optimum of both combined responses is located at pH 7.5 and 25.0 °C.

	Suggested experimental conditions		Predicted optimal conditions		
Iteration	**pH**	**Temperature**	**pH**	**Temperature**	***NPP*** **[%]**
1	6.56	20.71	-	-	-
2	6.85	35.81	-	-	-
3	8.05	13.63	-	-	-
4	8.77	33.34	-	-	-
5	7.20	15.88	6.72	18.05	72.81
6	9.07	21.75	6.62	16.53	67.99
7	7.69	26.75	7.68	26.67	93.59
8	6.85	27.28	7.51	25.55	98.41
9	7.93	39.75	7.55	25.22	98.65
10	7.42	23.18	7.58	24.92	98.08
11	7.30	29.67	7.59	24.84	97.81
12	5.84	42.20	7.61	24.74	97.28
13	7.92	23.02	7.51	25.09	99.65
14	9.36	42.20	7.52	25.12	99.41
15	7.49	25.07	7.52	25.13	99.40
16	7.46	25.14	7.51	25.13	99.56
17	7.56	25.45	7.51	25.13	99.56
18	7.53	25.16	7.50	25.12	99.66
19	7.53	24.93	7.50	25.13	99.63
20	5.68	11.54	7.50	25.09	99.74

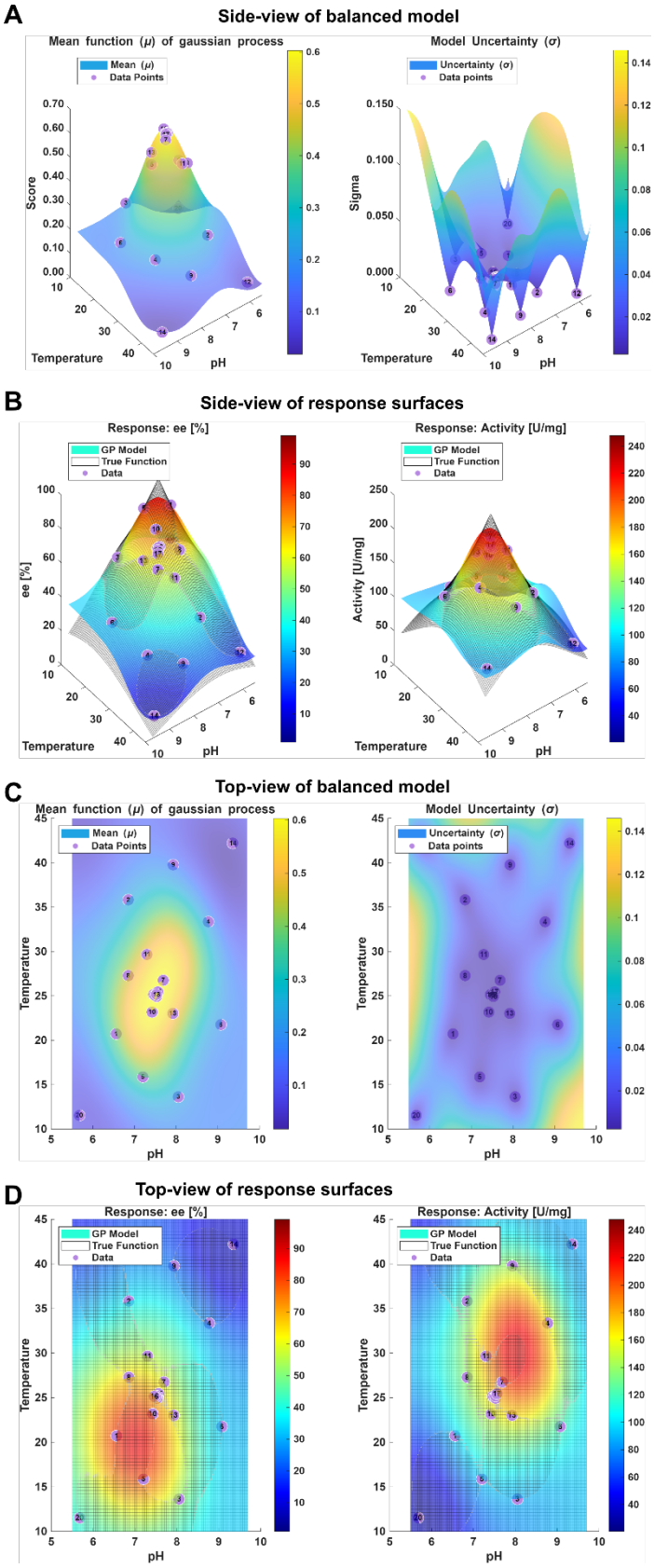

Figure S1. Exported figures after 20 iterations of BO of two overlapping smooth Ackley functions. Synthetic data was utilized according to **Table S6**, with the data points and the *NPPs* over the iterations are listed in **Table S7**. **A.** Side-view of balanced GP model controlled by the weight parameters, **B.** Side-view of the response surfaces of the *ee* and the activity, **C.** Top-view of the balanced GP model and **D:** Top-view of the response surfaces.

1.9.2.2 Random Gaussian noise application to smooth Ackley functions

To simulate experimental variance, Gaussian noise was superimposed onto the synthetic function values of the previous case **(Table S6)**. The noise standard deviation (σ) was derived from a target Signal-to-Noise Ratio (SNR_{dB}) relative to the maximum theoretical signal ($S_{\max}$), as defined by **equation (S6).**[70]

$$\sigma_{noise} = \frac{S_{\max}}{10^{\left(\frac{SNR_{dB}}{20}\right)}} \tag{S6}$$

The stochastic component was implemented by scaling a random variable sampled from a standard normal distribution ($\mathcal{N}(0,1)$), mimicking realistic uncertainties of measurements in chemical assays or reactions. We compared the influence of random Gaussian SNR_{dB} until the failure point of the optimizer, where the response surface of the synthetic function was not fitted correctly. The accuracy of the BO-script is visualized in **Figure S2** with the development of the *NPP* over 20 iterations. With no noise applied the optimizer achieved 99.74% overlap with balanced target value. As failure point, we identified 10 dB of SNR_{dB} (31.6% SNR amplitude: 3.16:1), with the BO-script not being able to successfully plot both responses (**Figure S2, C)**. Although with 10 dB of SNR_{dB} applied, the BO-script still reached an *NPP* value of 83.75%.

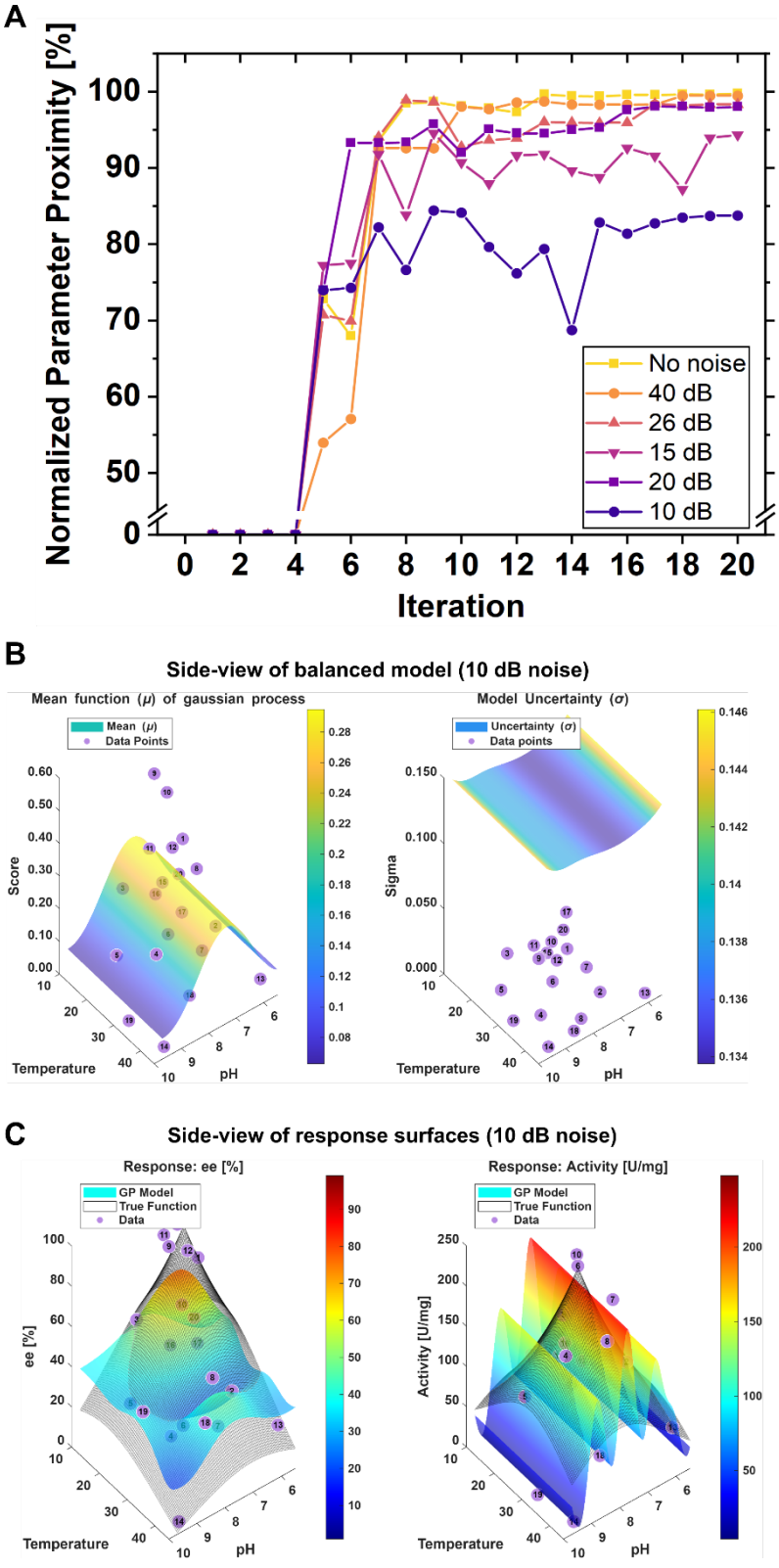

Figure S2. A. *NPP* over 20 iterations of different SNR values applied to the two overlapping smooth Ackley functions of previous case **(Table S6)**. Exported figures after 20 iterations with 10 dB of noise identified as failure point of the BO script (mean of three runs). **B.** Side-view of the balanced GP model and the model uncertainty. **C.** Top-view of the response surfaces (color plot) stacked with actual synthetic functions to be optimized (mesh plot).

1.9.2.3 Different test functions applied for the responses to be optimized

To further complicate the fitting for the optimizer, we utilized a different test function for each response to be optimized, as last presented validation test for the BO-script. We utilized a modified Rastrigin function[71] according to **equation (S7)** and a modified Rosenbrock function[72] according to **equation (S8)** for the response value calculation, where the modification $dx = x - x_t$ and $dy = y - y_t$ enables shifting of the optimum in the script settings. The parameter settings for the synthetic data is described in **Table S8.** The experimental settings over 20 iterations and the predicted maximum of the balanced GP-model is listed in **Table S9**. The NPP of the GP-models of both responses in comparison to the balanced model is visualized over 20 iterations in **Figure S3 A**. In this similar case to the previous utilization of randomized Gaussian noise, the *NPP* values of the GP-model prediction of the first response applying a Rastrigin function, the optimizer shows accurately the functions maximum (*NPP* of 95.3% after 20 iterations). As the Rosenbrock function has a large area close to the theoretical maximum, our BO-script calculates low *NPP* values for this specific response (*NPP* of 54.1% after 20 iterations). Although as both responses are combined in the balanced model and the activity response is dynamically normalized to its highest data point, the prediction of the balanced optimal conditions is not compromised by the low *NPP* values of the activity response. The calculated response surfaces of the different GP-models are shown along the uncertainty of the balanced model in **Figure S3 B, C**.

$$f(x,y)_{\text{Rastrigin}} = a \cdot 2 + [dx^2 - a\cos(2\pi(dx)] + [dy^2 - a\cos(2\pi(dy)] \quad \text{(S7)}$$

$$f(x,y)_{\text{Rosenbrock}} = (a - (dx + a))^2 + b((dy + a^2) - (dx + a)^2)^2 \quad \text{(S8)}$$

Table S8. Parameter setting for the optimization of a Rastrigin and a Rosenbrock function. Randomized noise was not applied.

***ee* function: Rastrigin, maximum at pH 8, 30 °C**	**Max. value = 100; *a* = 5**
Activity function: Rosenbrock, maximum at pH 8, 30 °C	Max. value = 250; *a* = 1, *b* = 100

Table S9. Experimental settings over 20 iterations and the predicted maximum of the current balanced GP-model after the initial data points by LHS. Synthetic data was utilized according **Table S8**. The balanced optimum of both combined responses is located at pH 8.0 and 30 °C.

	Suggested experimental conditions		Predicted optimal conditions		
Iteration	**pH**	**Temperature**	**pH**	**Temperature**	***NPP*** **[%]**
1	7.20	18.86	-	-	-
2	6.15	24.52	-	-	-
3	9.09	30.32	-	-	-
4	7.98	41.17	-	-	-
5	7.94	15.32	7.98	41.17	68.08
6	7.98	34.10	7.98	33.40	90.27
7	7.98	27.07	7.98	27.07	91.62
8	6.45	15.29	7.96	29.58	98.47
9	7.23	30.53	7.75	28.70	92.98
10	5.84	42.20	7.76	28.72	93.22
11	9.36	18.20	8.01	28.87	96.76
12	9.34	41.98	8.00	28.99	97.11
13	7.48	26.67	7.93	30.33	98.09
14	8.32	30.53	7.87	30.20	96.85
15	7.85	29.76	7.90	30.43	97.32
16	7.96	30.02	7.90	30.47	97.27
17	7.92	30.25	7.90	30.40	97.36
18	5.69	11.60	8.09	31.09	96.22
19	6.75	43.58	8.09	31.01	96.41
20	9.53	32.88	8.11	31.05	96.02

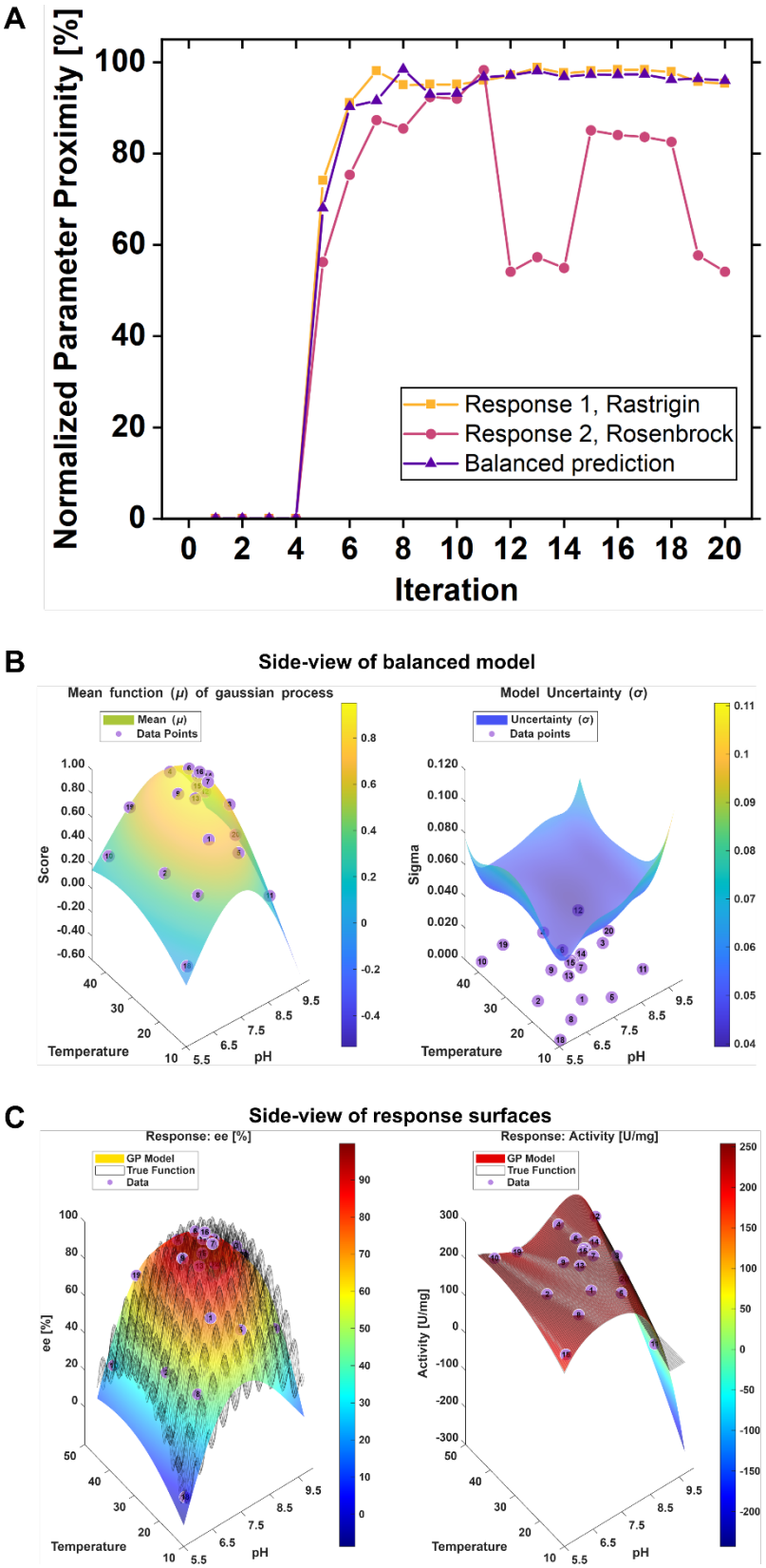

Figure S3. A. *NPP* over 20 iterations of the GP-models of both responses in comparison to the balanced model. A Rastrigin function was set for the first response (*ee*) and a Rosenbrock function for the second response to be optimized, with the parameter settings listed in **Table S8**. Exported figures after 20 iterations of optimization. **B.** Side-view of the balanced GP model and the model uncertainty. **C.** Side-view of the predicted response surfaces (color plot) stacked with actual synthetic functions to be optimized (mesh plot).

1.9.3 Experimental BO of RBR conditions utilizing the BO-MATLAB script

The BO of RBR conditions was carried out in a factorial range of pH 5.5–9.7. This required the utilization of different biological buffer systems (MES, MOPS, HEPES, and AMPSO). The pH ranges are visualized in **Figure S5**, with the black frame indicating the planned choice of buffer system, regarding their overlap. TRIS-HCl buffer was utilized in previous studies on AMDase and is therefore shown in comparison. Further, in **Section 3.2** the effect of buffer choice was determined, indicating a lower activity of *Bb*AMDase in TRIS-HCl buffer compared to HEPES and MOPS buffer at pH 7.8. The slight alkaline pH range was covered by AMPSO buffer. While neither AMPSO nor TRIS-HCl is classified as Good's buffers, no detrimental effects on AMDase activity were observed during this study. Both buffers possess structures capable of tri-dentate metal ion chelation, as visualized in **Figure S4.** While no chelation from buffer components to loaded metal ions on the IMA carrier were observed in this study, such complexation could potentially interfere with affinity-based immobilization.

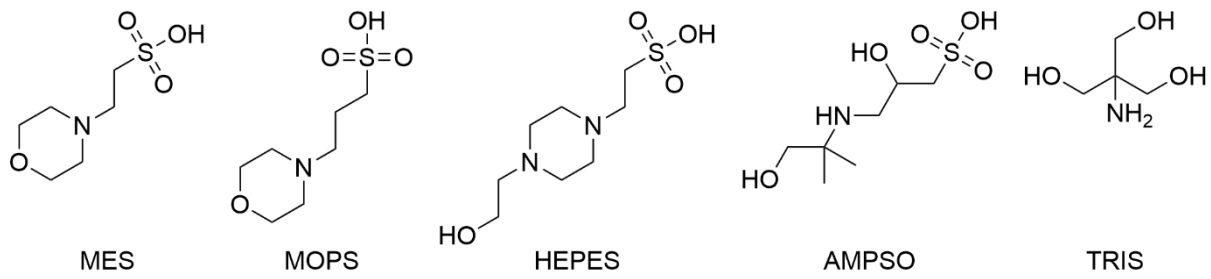

Figure S4. Structural comparison of buffers utilized for the biocatalytic decarboxylation by AMDase in this and previous studies.

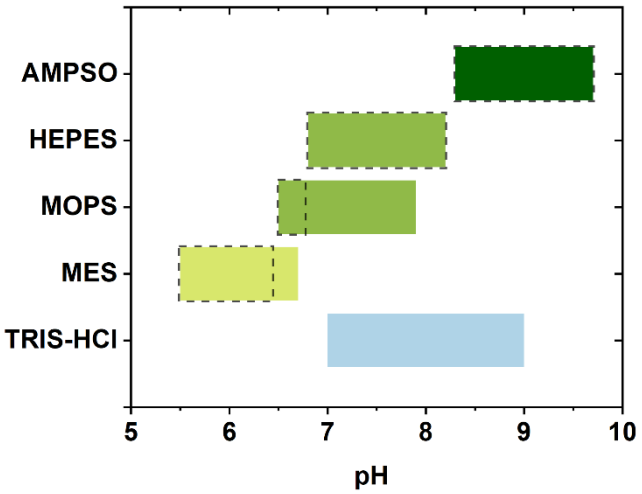

Figure S5. Biological buffer systems with their pH range visualized. The boxes around the respective buffers show the planned choice of buffer system during the Bayesian optimization of RBR conditions (The HEPES buffer was utilized in its full pH range; the MOPS buffer was utilized from its lower pH range instead of the MES buffer). The TRIS-HCl buffer (lowest row, blue) was not utilized regarding the lower activity of the free enzyme in this respective buffer determined in **Section 3.2**.

Table S10. Experimental settings of the experimental Bayesian optimization of RBR conditions. The choice of the buffer system with their respective ranges is visualized in **Figure S5**.The initial specific activity was determined based on the enzyme carrier utilized, with the procedure described in **Section 3.4**. The enantiomeric excess was determined after >99% conversion was determined by HPLC-DAD. Therefore, the produced (*S*)-Flurbiprofen (**2c**) was extracted from the acidified sample (1 mL) with EtOAc and analyzed by chiral GC according to **Section 2.2** and **Section 2.3**.

Experiment	Temperature	pH	Buffer system	Specific activity [U/$g_{carrier}$]	*ee* [%]
1	32.7	8.2	HEPES	28.2	99.0
2	40.0	5.6	MES	30.1	97.6
3	24.4	6.7	MOPS	25.6	98.3
4	15.4	9.3	AMPSO	22.6	99.5
5	35.3	8.7	AMPSO	27.5	99.6

The current model predictions after the five experimental data points (**Table S10**) are summarized in **Table S11**. The GP-model of the enantiomeric excess (*ee*) suggests the highest *ee* value at pH 8.9 and 35.3 °C, while the activity is maximized at the design's corner (pH 5.5 and 45.0 °C). The calculated maximum of the balanced GP-model is shifted towards the maximized activity by the normalization approach described above in the beginning of **section 1.9** and the equal '*weights*' parameters (*ee*: 0 to100%, activity: 0 to highest observed entry).

Our BO-script allows the proactive assessment of the optimization after loading previous results from a *csv* file and every BO iteration. The script is recalculating the maximum of both individual response surfaces and the combined GP-model. This allows the optimization process to be terminated at any point once a satisfactory response is achieved or resources are depleted.

Table S11. Suggested optimal conditions after five experimental entries into the BO-script. The suggestions are the calculated maxima of the internal '*bayesopt'* GP-models of both responses and the combined GP-model, as described in **Section 1.9**. The predicted result for the responses equals the value of the GP-functions maximum in the respective design space.

Model	Temperature	pH	Predicted result
Balanced	45.0	5.6	-
Activity	45.0	5.5	30.4 U/mg
ee	35.3	8.9	99.7%

2 Analytical methods

2.1 HPLC measurements

HPLC samples were measured on an Agilent Technologies 1100 Series HPLC device (Agilent Technologies) equipped with a DAD detector (210 nm). For the measurement of aryl-propionic acids and their corresponding malonic acids a Kinetex® 2.6 µm Polar C18 column (RP, 100 Å, 150 × 4.6 mm) was utilized with **HPLC Method 1**. For the measurement of alkyl-butenoic acids and their corresponding malonic acids an Agilent Zorbax® 3.5 µm C8 column (RP, 4.6 x 75 mm) was utilized with **HPLC Method 2**.

HPLC Method 1: 1 mL/min flow rate, 40 °C column temperature, 20 mM H_3PO_4 aq. / ACN, 95/5 → 20/80,10 min; 20/80,2 min; 95/5, 4 min.

HPLC Method 2: 1 mL/min flow rate, 40 °C column temperature, 20 mM H_3PO_4 aq. / ACN, 95/5 → 20/80,10 min; 20/80,2 min; 95/5, 4 min.

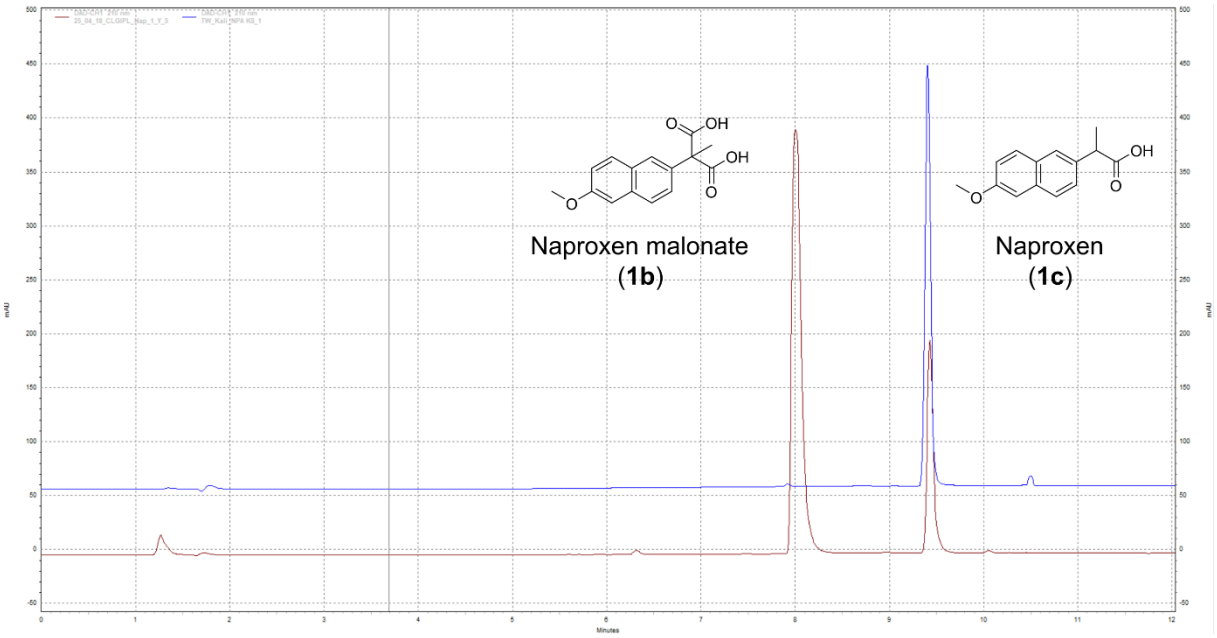

Figure S6. Exemplary HPLC chromatogram of the biocatalytic conversion of naproxen malonate (brown) superimposed with the measurement of one calibration standard of naproxen (blue) at 210 nm. Retention times: naproxen malonate = 8.0 min, naproxen = 9.5 min.

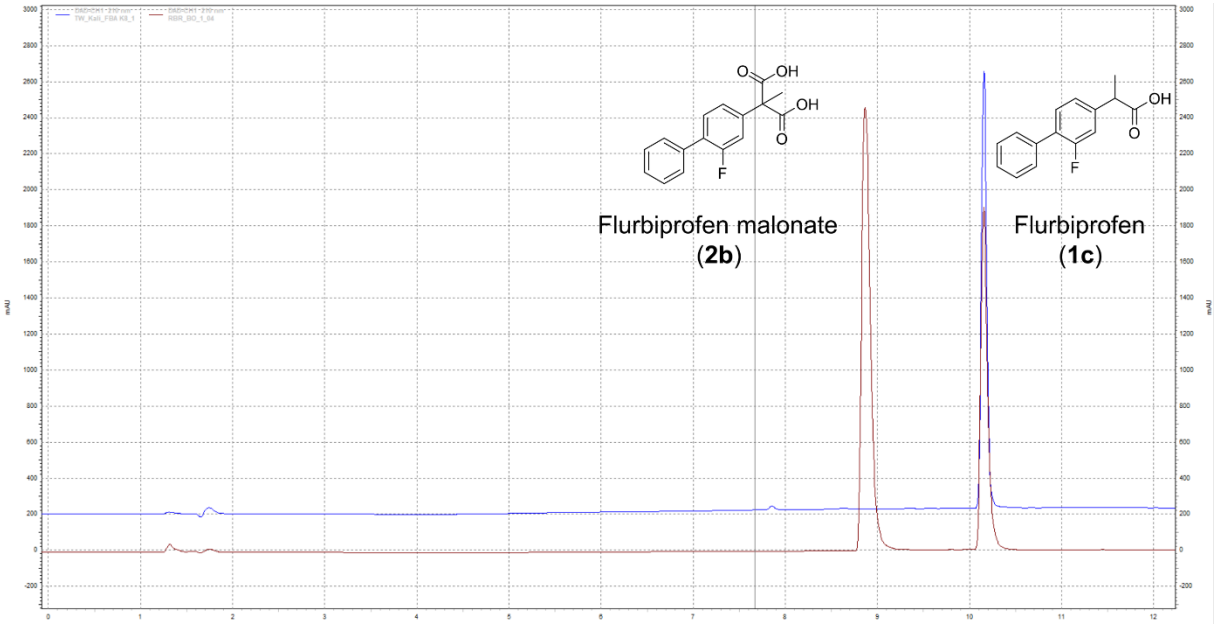

Figure S7. Exemplary HPLC chromatogram of the biocatalytic conversion of flurbiprofen malonate (brown) superimposed with the measurement of one calibration standard of flurbiprofen (blue) at 210 nm. Retention times: flurbiprofen malonate= 8.9 min, flurbiprofen = 10.2 min.

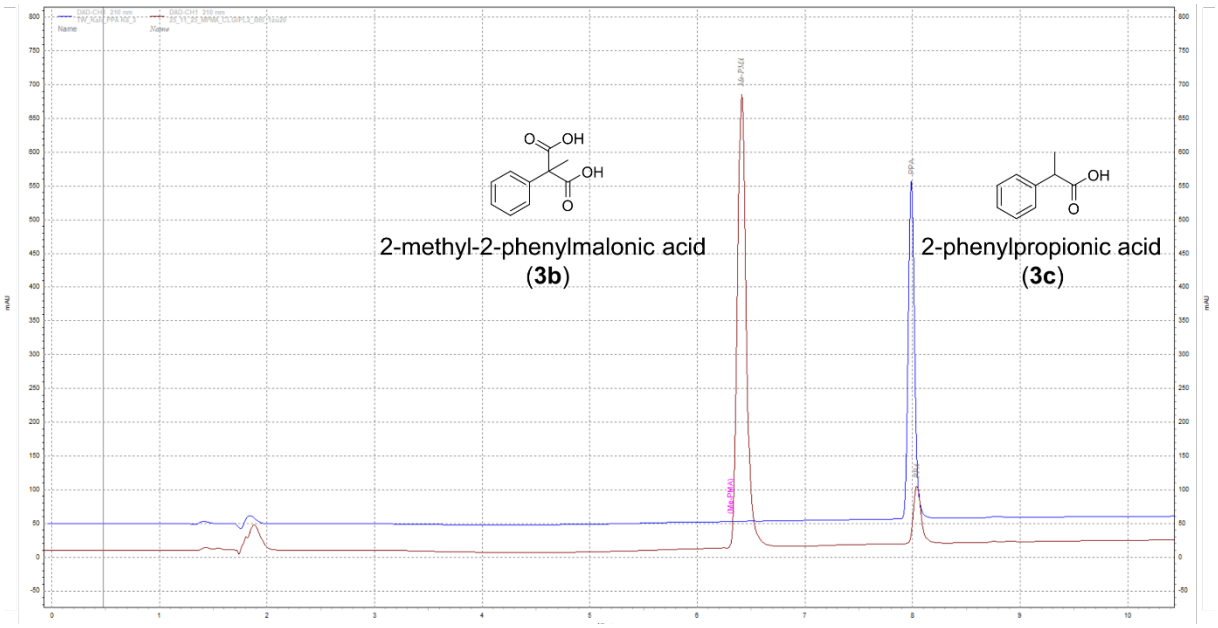

Figure S8. Exemplary HPLC chromatogram of the biocatalytic conversion of 2-methyl-2-phenylmalonic acid (brown) superimposed with the measurement of one calibration standard of 2-phenylpropionic acid (blue) at 210 nm. Retention times: 2-methyl-2-phenylmalonate = 6.4 min, 2-phenylpropionic acid = 8.0 min.

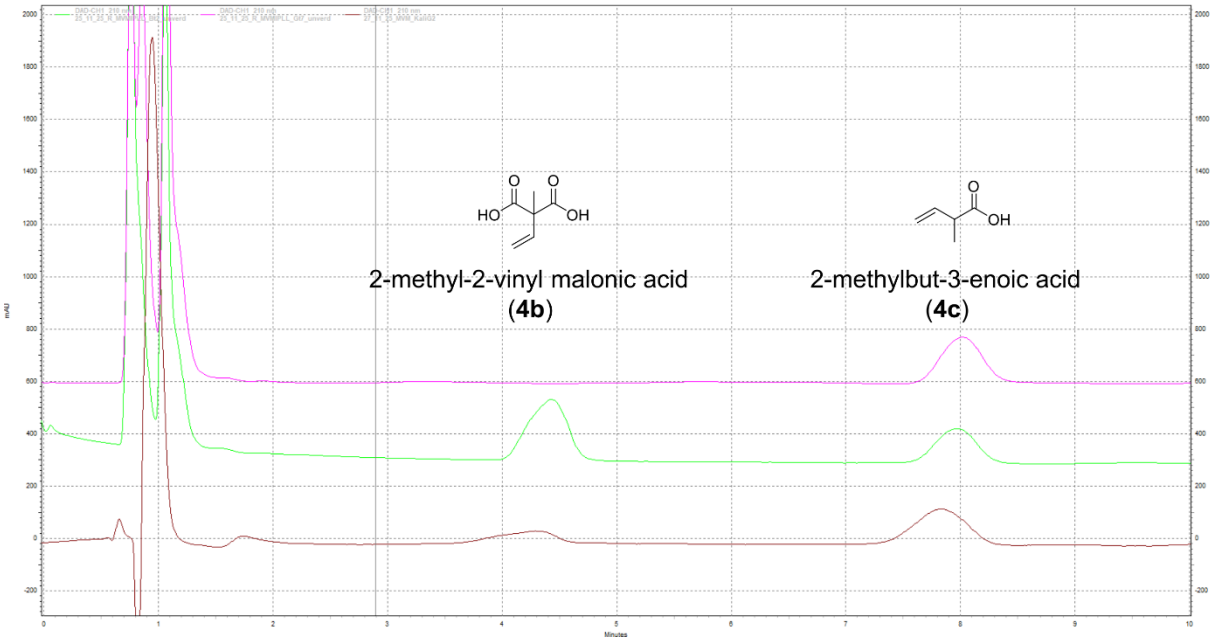

Figure S9. Exemplary HPLC chromatogram of the biocatalytic conversion of 2-methyl-2-vinylmalonic acid (green, middle) superimposed with the measurement of one calibration standard (brown, bottom) containing both substrate and product, and the last data point of the preparative scale conversion of **4b** (pink, top) at 210 nm. Retention times: 2-methyl-2-vinylmalonic acid = 4.4 min, 2-methylbut-3-enoic acid = 7.9 min.

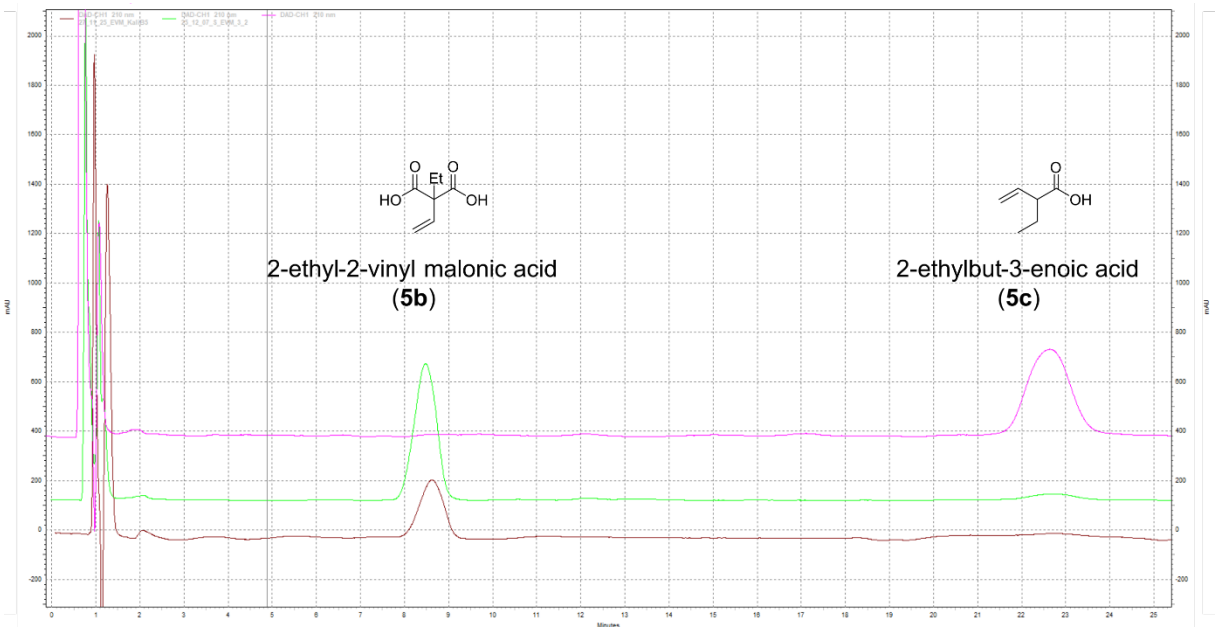

Figure S10. Exemplary HPLC chromatogram of the biocatalytic conversion of 2-ethyl-2-vinylmalonic acid (green, middle) superimposed with the measurement of one calibration standard (brown, bottom) of the substrate, and the last data point of the preparative scale conversion of **5b** (pink, top) at 210 nm. Retention times: 2-ethyl-2-vinylmalonic acid = 8.6 min, 2-ethylbut-3-enoic acid = 22.7 min.

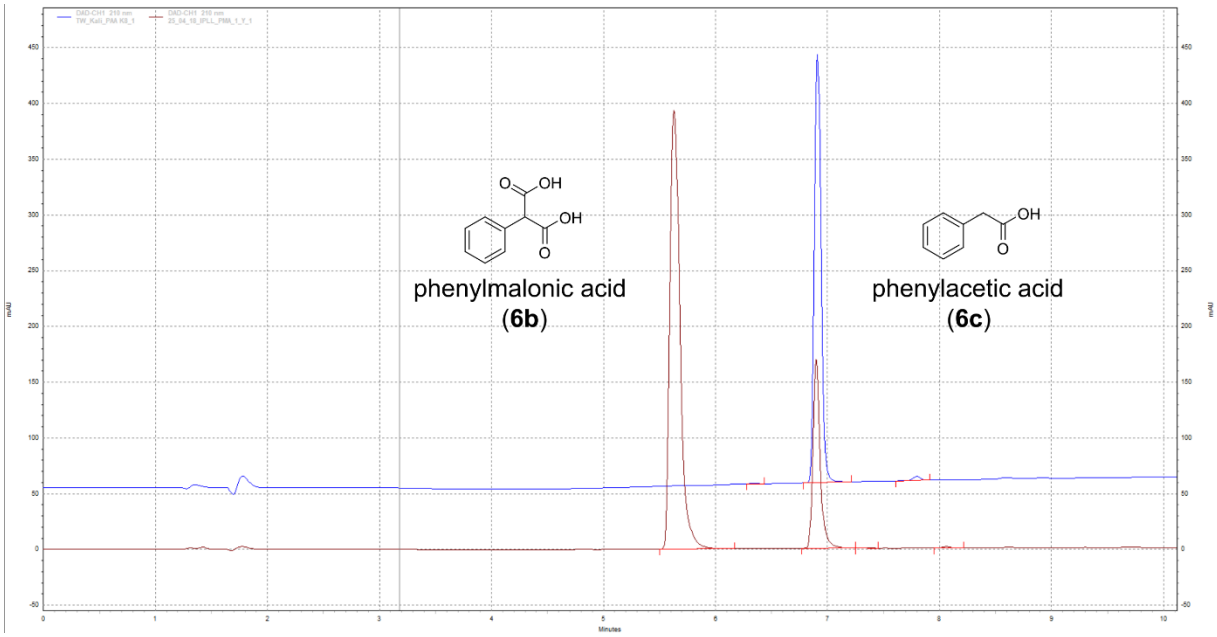

Figure S11. Exemplary HPLC chromatogram of the biocatalytic conversion of phenylmalonic acid (blue) superimposed with the measurement of one calibration standard of phenylacetic acid (blue) at 210 nm. Retention times: phenylmalonate = 5.7 min, phenylacetic acid = 6.9 min.

2.2 Derivatization for the determination of selectivity

For the determination of selectivity via chiral GC-FID, the reaction mixtures of aryl propionic acids were derivatized after >99% conversion was identified by HPLC-DAD. Therefore, a 1 mL sample was acidified with HCl (4 M, 200 µL), extracted with 300 µL EtOAc and dried with anhydrous magnesium sulfate. The sample was mixed with 100 µL MeOH and 25 µL TMS-CH_2-N_2 and incubated (30 min, 22 °C). The derivatization was terminated with 2.5 µL anhydrous acetic acid and was dried in a stream of nitrogen.

The sample was dissolved in 200 µL EtOAc for GC analysis in a triplicate of different split ratios (10, 25, 50). 2-alkyl-butenoic acids were analyzed directly after the extraction and drying of the sample with anhydrous magnesium sulfate.

2.3 Chiral GC measurements

Chiral GC FID samples were measured on a Shimadzu Nexis GC-2030 device equipped with an AOC-20i/s 208 autosampler using a Macherey-Nagel cyclodextrin column (Hydrodex-β-6TBDM. Chiral stationary phase, 25 m, 0.25 mm ID, 0.25 µm df). An isothermal method was used for each product to achieve baseline separation. Peak identification of products **1c**–**5c** was done in reference to literature.[15,16,36,73]

SPL1: Injection volume: 1 µL, Injection mode: split, Injection temperature: 250 °C, Carrier Gas: H_2, Flow control mode: Linear velocity. **Column:** Wash ramp:10 °C/min until 210 °C, 1 min hold time. **FID:** Sampling Rate 40 ms, Makeup Gas: H_2, Detection Temperature: 230 °C, Makeup Flow 24.0 mL/min, H_2 Flow: 32.0 mL/min, Air Flow 200.0 mL/min.

Naproxen-methylester: SPL1: Linear Velocity: 40 cm/s, **Column:** Temperature: 165 °C, Hold Time: 90 min.

Flurbiprofen-methylester: SPL1: Linear Velocity: 40 cm/s, **Column:** Temperature: 160 °C, Hold Time: 65 min.

Methyl 2-phenylpropanoate: SPL1: Linear Velocity: 20 cm/s, **Column:** Temperature: 100 °C, Hold Time: 30 min.

2-Methylbut-3-enoic acid: SPL1: Linear Velocity: 80 cm/s, **Column:** Temperature: 70 °C, Hold Time: 45 min.

2-Ethylbut-3-enoic acid: SPL1: Linear Velocity: 85 cm/s, **Column:** Temperature: 90 °C, Hold Time: 30 min.

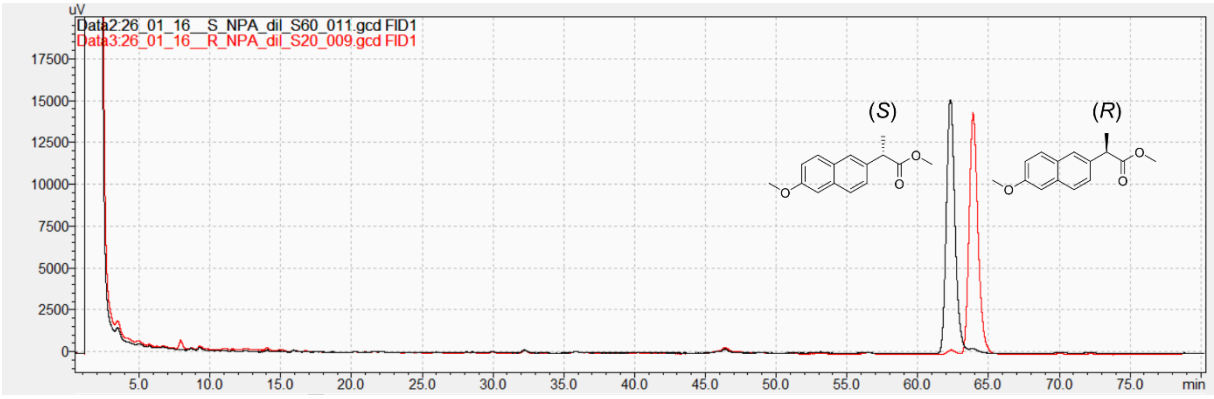

Figure S12. Exemplary GC-FID chromatogram of the converted naproxen malonate with (*S*)-selective AMDase ICPLLG (black) superimposed with (*R*)-selective AMDase IPLL (red). The samples were derivatized with TMS-CH_2-N_2 according to **Section 2.2.** Retention times: (*S*)-Naproxen-methylester = 62.4 min, (*R*)-Naproxen-methylester = 64.0 min.

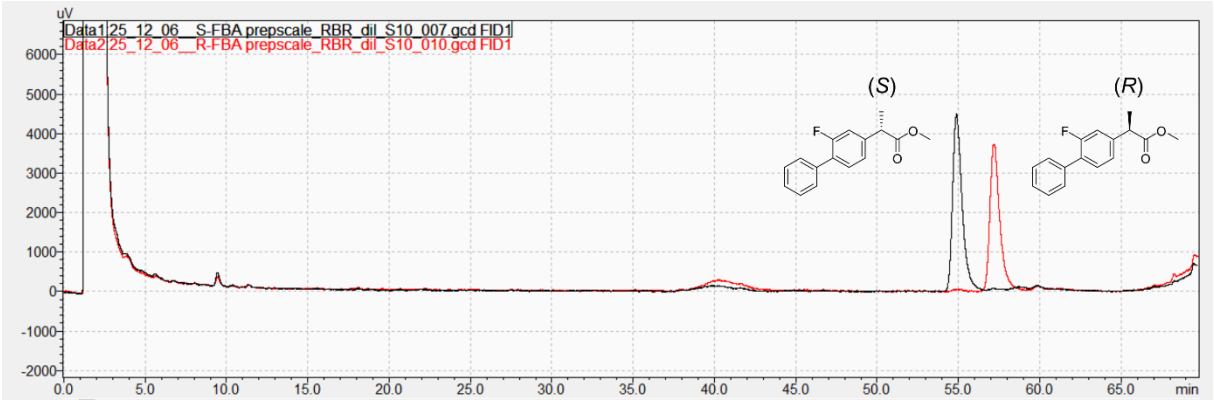

Figure S13. Exemplary GC-FID chromatogram of the converted flurbiprofen malonate with (*S*)-selective AMDase ICPLLG (black) superimposed with (*R*)-selective AMDase IPLL (red). The samples were derivatized with TMS-CH_2-N_2 according to **Section 2.2**. Retention times: (*S*)-flurbiprofen-methylester = 55.0 min, (*R*)-flurbiprofen-methylester = 57.4 min.

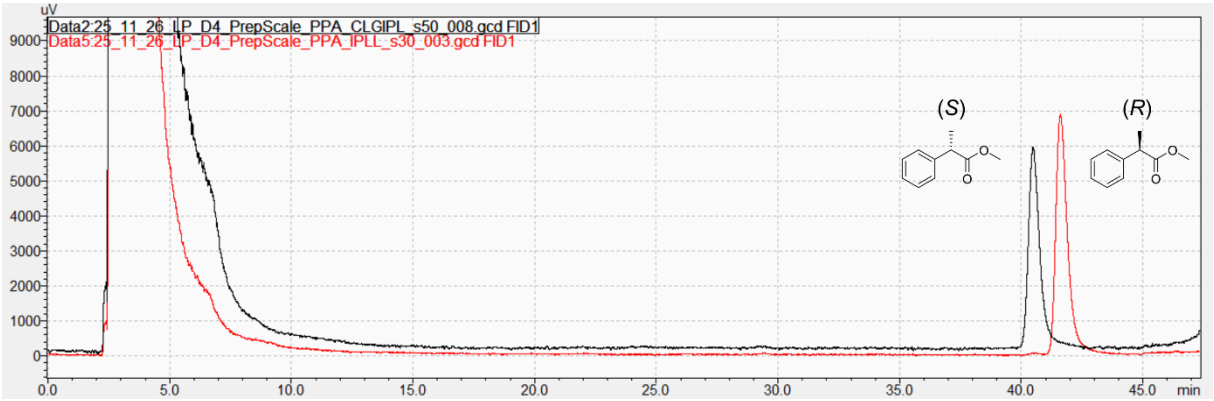

Figure S14. Exemplary GC-FID chromatogram of the converted 2-methyl-2-phenylmalonate with (*S*)-selective AMDase ICPLLG (black) superimposed with (*R*)-selective AMDase IPLL (red). The samples were derivatized with TMS-CH_2-N_2 according to **Section 2.2**. Retention times: methyl (*S*)-2-phenylpropanoate = 40.5 min, methyl (*R*)-2-phenylpropanoate = 41.6 min.

For both vinylic compounds **4c** and **5c** we could not establish our previously published baseline separation of the respective enantiomers using another GC setup. No baseline separation could be achieved neither while changing for the analytical method's conditions nor derivatization utilizing TMS-CH_2-N_2.

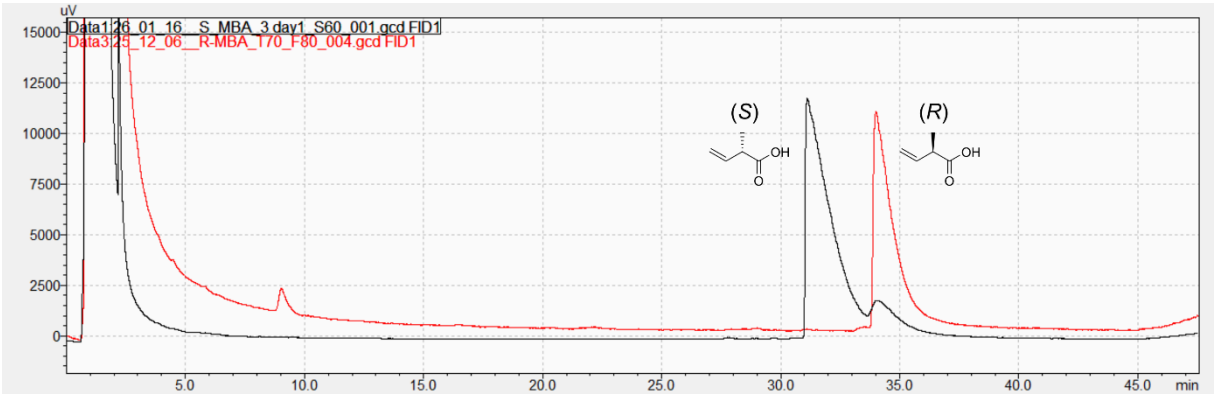

Figure S15. Exemplary GC-FID chromatogram of the converted 2-methyl-2-vinylmalonate with (*S*)-selective AMDase ICPLLG (black) superimposed with (*R*)-selective AMDase IPLL (red). Retention times: (S)-2-methylbut-3-enoic acid = 31.4 min, (*R*)-2-methylbut-3-enoic acid = 34.2 min.

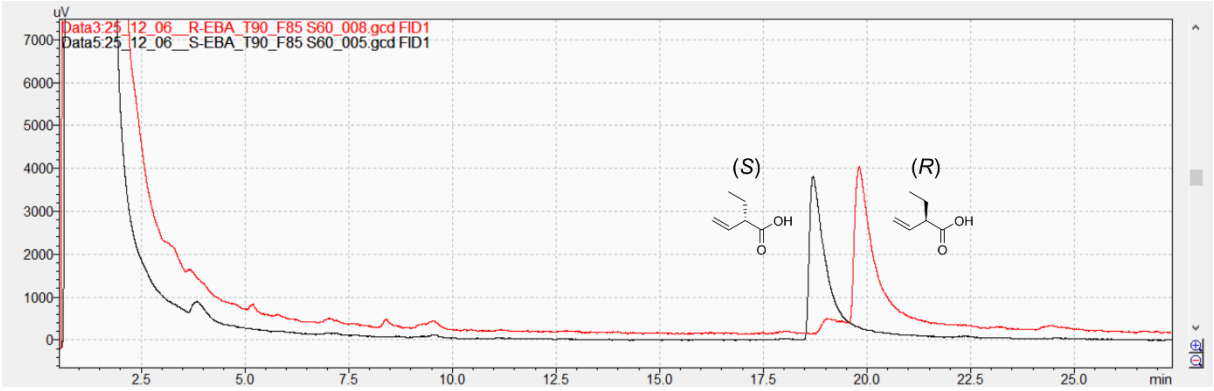

Figure S16. Exemplary GC-FID chromatogram of the converted 2-ethyl-2-vinylmalonate with (*S*)-selective AMDase ICPLLG (black) superimposed with (*R*)-selective AMDase IPLL (red). Retention times: (*S*)-2-ethylbut-3-enoic acid = 18.7 min, (*R*)-2-ethylbut-3-enoic acid = 19.8 min.

3 Experimental procedures

3.1 Preparation of cell-free extract (CFE)

The frozen cell pellet was thawed on ice and resuspended (75 mg/mL, 4 °C) in either HEPES buffer (50 mM, pH 8) or the respective binding buffer for immobilization (**Table S3, Table S4**). Cell lysis was achieved via sonication on ice (3 x 1 min cycle of 2 sec pulse and 8 sec pause,1 min break, 50% amplitude). The resulting lysate was then centrifugated (10,000 rpm, 4 °C, 30 min), and the supernatant was kept on ice until further use.

For the preparative scale reactions, the considerable larger cell pellet utilized was resuspended (200 mg/mL, 4 °C) and cell disruption was carried out utilizing a Microfluidics™ LM20 Microfluidizer®

(machine pressure value: 15.000 psi, 4 °C). The lysate was kept on ice and then centrifuged (2 h, 13.000 rpm, 4 °C). The supernatant was collected and used as CFE for the intensified immobilization for the preparative scale experiments.

3.2 Enzymatic activity of free AMDase

The effect of buffer choice was determined with the utilization of a 50 mM buffer preparation at pH 7.9. The following buffer systems have been used: TRIS-HCl, KPi, HEPES, and MOPS buffer. For the determination of the activity in ddH_2O the pH was not adjusted. The general procedure of activity determination is described in **section 3.4** and was carried out utilizing the CFE of *Bb*AMDase.

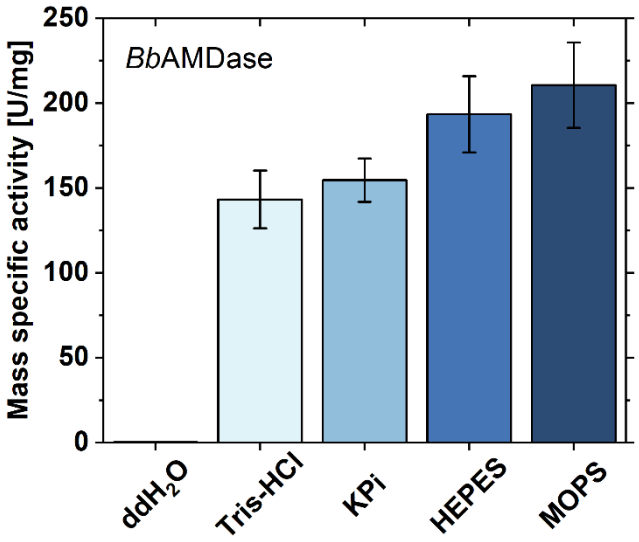

Figure S17. Effect of the choice of buffer system on the mass-specific activity [U/mg] utilizing CFE of *Bb*AMDase. All buffers were prepared in a concentration of 50 mM with adjustment to pH 7.9. No pH adjustment was carried out for ddH_2O (n=7).

3.3 Enzyme immobilization

Summarized characteristics of the enzyme carriers utilized in this study are listed in **Table S12**.

Table S12. Summary of the characteristics of the enzyme carriers utilized in this study provided by Seplife®. Information is based on the certificate of analysis (COA) of the respective carriers. Information on the pore size is obtained from Sunresin New Materials Co., Ltd. brochure of enzyme carriers. All carriers utilized are based on a polyacrylate matrix. Analyzed values of the COA are stated in brackets below the specified value of the product.

Product name	Functional	Type	Particle size [µm]	Pore size [Å]	Surface area (m^2/g)	Total moisture [%]	Capacity [mmol/g]
Chelex 7350S/Co^{2+}	Iminoacetic	Affinity	100–250 (90.2%)	800–1000	≥25	60–70 (65.4)	≥0.5 (1.4)
Chelex 7350S/Zn^{2+}	Iminoacetic	Affinity	100–250 (93.0%)	800–1000	≥25	60–70 (66.9)	≥0.5 (1.0)
Chelex 7350S/ Ni^{2+}	Iminoacetic	Affinity	100–250 (97.7%)	800–1000	≥25	60–70 (66.9)	≥0.5 (1.0)
Chelex 7350S/Fe^{2+}	Iminoacetic	Affinity	100–250 (97.3)	800–1000	≥25	60–70 (66.9)	≥0.4 (1.0)
Chelex 7350S/Cu^{2+}	Iminoacetic	Affinity	100–300 (97.7%)	800–1000	≥25	60–70 (66.9)	≥0.5 (1.0)
EMC7225S	Amino C2	Covalent	100–300 (96.1%)	500-700	≥120	60–70 (64.4)	≥0.4 (1.0)
EMC7120S	Amino C6	Covalent	100–300 (92.3%)	200-400	≥100	50–60 (55.9)	≥0.4 (0.8)

All carriers evaluated in this study were analyzed for biocatalyst leaching. Leaching was assessed using BCA protein quantification as well as activity measurements of the undiluted HEPES buffer employed for carrier suspension in the half-life determination experiments. In all cases, the amount of leached protein was below the detection limit of the BCA assay, or, when detectable, the protein content was lower than expected based on activity measurements. Consequently, only activity-based leaching data are summarized for the different carrier preparations in **Table S13**. Notably, no leaching was observed when glutaraldehyde was used as the crosslinking agent.

Table S13. Determined activity leaching of the evaluated enzyme carrier preparations. The immobilization procedure is described in **Section 3.3**. Activity leaching was determined after 4 h of incubation in 50 mM HEPES buffer (pH 8) and is calculated in percentage based on the respective protein loading of the carrier preparation.

AMDase ICPLLG		**AMDase IPLL**	
Carrier preparation	**Activity leaching [%]**	**Carrier preparation**	**Activity leaching [%]**
Chelex 7350S/Co^{2+}	2.3	Chelex 7350S/Co^{2+}	4.6
EMC7225S; amino C2-DFF	1.9	EMC7225S; amino C2-DFF	5.4
EMC7120S; amino C6-DFF	0	EMC7120S; amino C6-DFF	0
EMC7225S; amino C2-Glu	0	EMC7225S; amino C2-Glu	0
EMC7120S; amino C6- Glu	0	EMC7120S; amino C6- Glu	0

For the preparative scale reaction in the RBR, each batch of carrier preparation was utilized for the comparability of different experiments. The determined characteristics of the immobilized AMDase are summarized in **Table S14**. For the immobilization of AMDase IPLL, 180 g of Seplife® EMC7225S with glutaraldehyde as crosslinking agent was used, and for AMDase ICPLLG, 200 g.

Table S14. Enzyme characteristics of immobilized AMDase on Seplife® EMC7225S. Determined mass-specific activities based on the total protein amount of the CFE determined by BCA-assay. The initial activities are calculated towards phenylmalonic acid into phenylacetic acid at 30 °C in HEPES-buffer (50 mM, pH 8), as described in **Section 3.4**.

Enzyme variant	$a_{spec,carrier}$ **[U/$g_{carrier}$]**	a_{spec} **[U/mg_{AMDase}]**	Y_{immo} **[%]**	Y_{act} **[%]**
IPLL-AMDase	147.2 ± 12.4	3.45 ± 0.27	56.7	5.5 ± 0.4
ICPLLG-AMDase	59.7 ± 11.1	1.31 ± 0.24	62.7	9.2 ± 0.3

3.3.1 Enzyme immobilization on Seplife® Chelex7350 affinity resin

Affinity immobilization was performed using Seplife® Chelex7350 affinity resin. The resin was equilibrated by washing four times with the affinity immobilization buffer (50 mM HEPES, 50 mM NaCl 10 mM imidazole, pH 7.4) in a resin-to-buffer ratio of 1:2 (w/v). The CFE was freshly prepared in the affinity immobilization buffer and subsequently transferred into the immobilization vessel containing the designated amount of resin. The resulting slurry was incubated utilizing a Stuart rotator (4 °C, 4 h, 20 rpm). The carrier preparation was filtered and was washed, with all steps conducting a resin:buffer ratio of 1:4 (w/v). The resin was washed twice with affinity immobilization buffer, and once with the affinity washing buffer (50 mM HEPES, 500 mM NaCl, 10 mM imidazole, pH 7.4), followed up by another wash with the affinity immobilization buffer. Washing steps and supernatants were collected for protein quantification. The resin was used immediately or stored at 4 °C until further use. Immobilizations were carried out in triplicates for this study.

3.3.2 Enzyme immobilization on Seplife® EMC7225S and EMC7120S amino resin

Covalent enzyme immobilization with Seplife® EMC7225S and EMC7120S amino resin was carried out by this procedure. The resin was equilibrated by washing four times with the covalent immobilization buffer (50 mM HEPES, 50 mM NaCl, pH 6.8) in a resin-to-buffer ratio of 1:2 (w/v). Afterwards, the pre-activation of the amino resin was conducted by the addition of diformylfuran (DFF) or glutaraldehyde (Glu) (1.05 eq. of NH_2-groups on the resin) to the immobilization buffer (50 mM HEPES, 50 mM NaCl, pH 6.8) in a resin-to-buffer ratio of 1:8 (w/v). The slurry was inverted utilizing a Stuart rotator (22 °C, 60 min, 20 rpm). The CFE was freshly prepared in the affinity immobilization buffer and subsequently transferred into the immobilization vessel containing the designated amount of resin. The resulting slurry was incubated utilizing a Stuart rotator (4 °C, 18 h, 20 rpm). The carrier preparation was filtered and was washed, with all steps conducting a resin:buffer ratio of 1:4 (w/v). The resin was washed twice with the covalent immobilization buffer, and once with the covalent washing buffer (50 mM HEPES, 500 mM NaCl, pH 6.8) followed by a final washing step with covalent immobilization buffer. The supernatant of all steps was collected for protein quantification. The resin was used immediately or stored at 4 °C until further use. Immobilizations were carried out in triplicates for this study.

3.4 Determination of initial activity

The initial activity of AMDase CFE or carrier preparations were determined in a range of 10% substrate conversion over 5 minutes. As indicated in the respective experiment 50 mM buffer preparation (pH 8) was utilized for all dilution steps. The freshly prepared CFE (100 µL, 0.3–0.5 mg/mL total protein after 10x dilution) was added to the incubated (30 °C, 600 rpm) substrate solution (final concentration: phenylmalonate (**6b**): 20 mM in 50 mM buffer preparation, pH 8). In case of determining the activity of immobilized AMDase, the carrier preparation was weighed in a reaction tube and the incubated substrate solution was added (30 °C, 1000 rpm). The conversion was determined by taking samples (100 µL at 0.15, 1.15, 2.15, 3.15, and 4.15 minutes), which are terminated by the sample's addition into ACN / H_2O (9:1, 200 µL). The samples were centrifugated (13,000 rpm, 4 °C, 20 min) and measured by HPLC-DAD at 210 nm. The mass-specific activity (U/mg) was calculated based on the quantified enzyme concentration by BCA-assay or the utilized mass of enzyme carrier.

The mass specific activity of the carrier preparation $a_{\mathrm{spec,carrier}}$ was calculated by **equation (S9)** with the determined activity a in zero-order kinetics and the mass of the carrier preparation m_{carrier}.

$$a_{\mathrm{spec,carrier}} = \frac{a}{m_{\mathrm{carrier}}} \tag{S9}$$

The immobilization yield Y_{immo} was calculated by **equation (S10)** based on the initial amount of total protein in the CFE P_{CFE} and the amounts of total protein P remaining in the supernatant (P_{S}) and wash fractions (P_{W}) determined by BCA-assay. The activity yield Y_{act} was calculated by **equation (S11)** based on the mass specific activity of immobilized protein $a_{\mathrm{spec,immo}}$ and the relative activity of the CFE ($a_{\mathrm{spec,CFE}}$) that was applied for immobilization.

$$Y_{\text{immo}} = \frac{P_{\text{CFE}} - P_{\text{S}} - P_{\text{W}}}{P_{\text{CFE}}} \cdot 100\% \quad \text{(S10)}$$

$$Y_{\text{act}} = \frac{a_{\text{spec,immo}} \cdot m_{\text{carrier}}}{a_{\text{spec,CFE}} \cdot P} \cdot 100\% \quad \text{(S11)}$$

3.5 Determination of half-life of carrier preparations

For the comparison of half-life of the immobilized enzyme preparations, samples were incubated at 30 °C under storage conditions. For this 1.5 mL tight seal micro centrifuge tubes containing 1 mL HEPES-buffer (50 mM, pH 7.8) were utilized. For the determination of activity at a given time, the carrier was suspended by inversion and 100 µL of the suspension was collected with a 1000 µL pipette with cut-off pipette tip. The retrieved aliquots were filtered and weighted in 2 mL reaction tube for the determination of activity as described in **section 3.4**. Left-over resin was resuspended in 100 µL HEPES and transferred back. The carrier preparations were subsequently incubated further.

The observed total turnover numbers (*TTN*) were calculated in reference to Bommarius *et al.* with **equations (S12)**–**(S14)**.[50]

$$k_{cat,obs}\ (s^{-1}) = \frac{specific\ activity\ (\text{U mg}^{-1}) \cdot enzyme\ molecular\ mass\ (\text{g mol}^{-1})}{60\,000} \quad \text{(S12)}$$

$$k_{d,obs}\ (\text{s}^{-1}) = \frac{\ln(2)}{half\ life} \quad \text{(S13)}$$

$$TTN = \frac{k_{cat,obs}\ (\text{s}^{-1})}{k_{d,obs}\ (\text{s}^{-1})} \quad \text{(S14)}$$

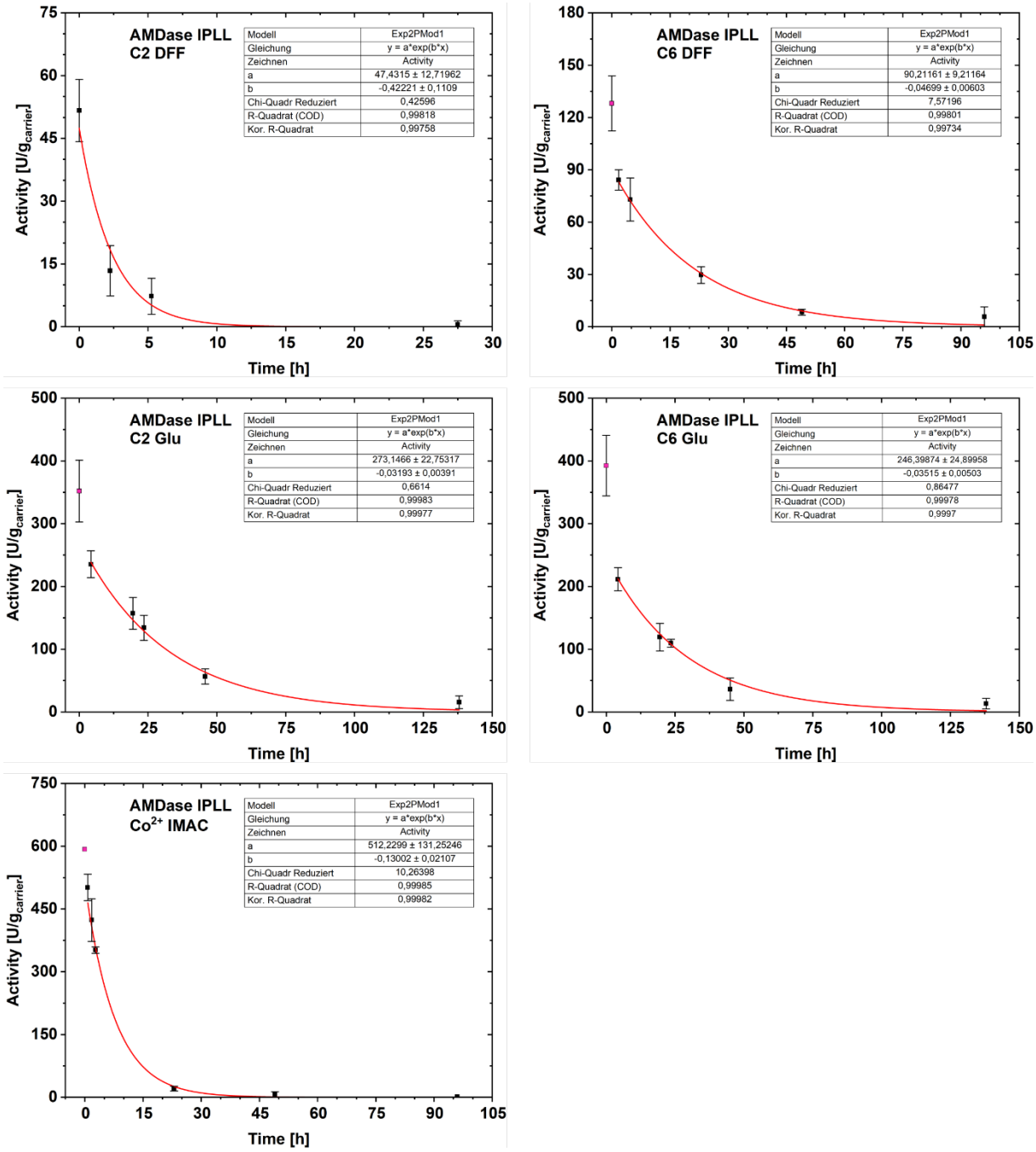

Figure S18. Time-course of the initial mass-specific activities of the AMDase IPLL variant immobilized onto different enzyme carriers. The different carriers utilized in this study are specified in **Section 3.3**. Fitting of data points was carried out in Origin with an exponential decay function. Initial data-points (highlighted in pink) show profound enzyme deactivation were excluded. Immobilization was carried out in triplicates (188–291 mg_{CFE},p/$g_{carrier}$), protein was quantified via BCA-assay. The initial activity of the carrier preparation was determined according to **Section 3.4**. Technical triplicates; 1 mL PMA-reaction-buffer (20 mM phenylmalonic acid (**6b)**, 50 mM HEPES, pH 7.8); 5 $mg_{carrier}$; 950 rpm, 30°C, 4.25 min total assay time, sampled each minute.

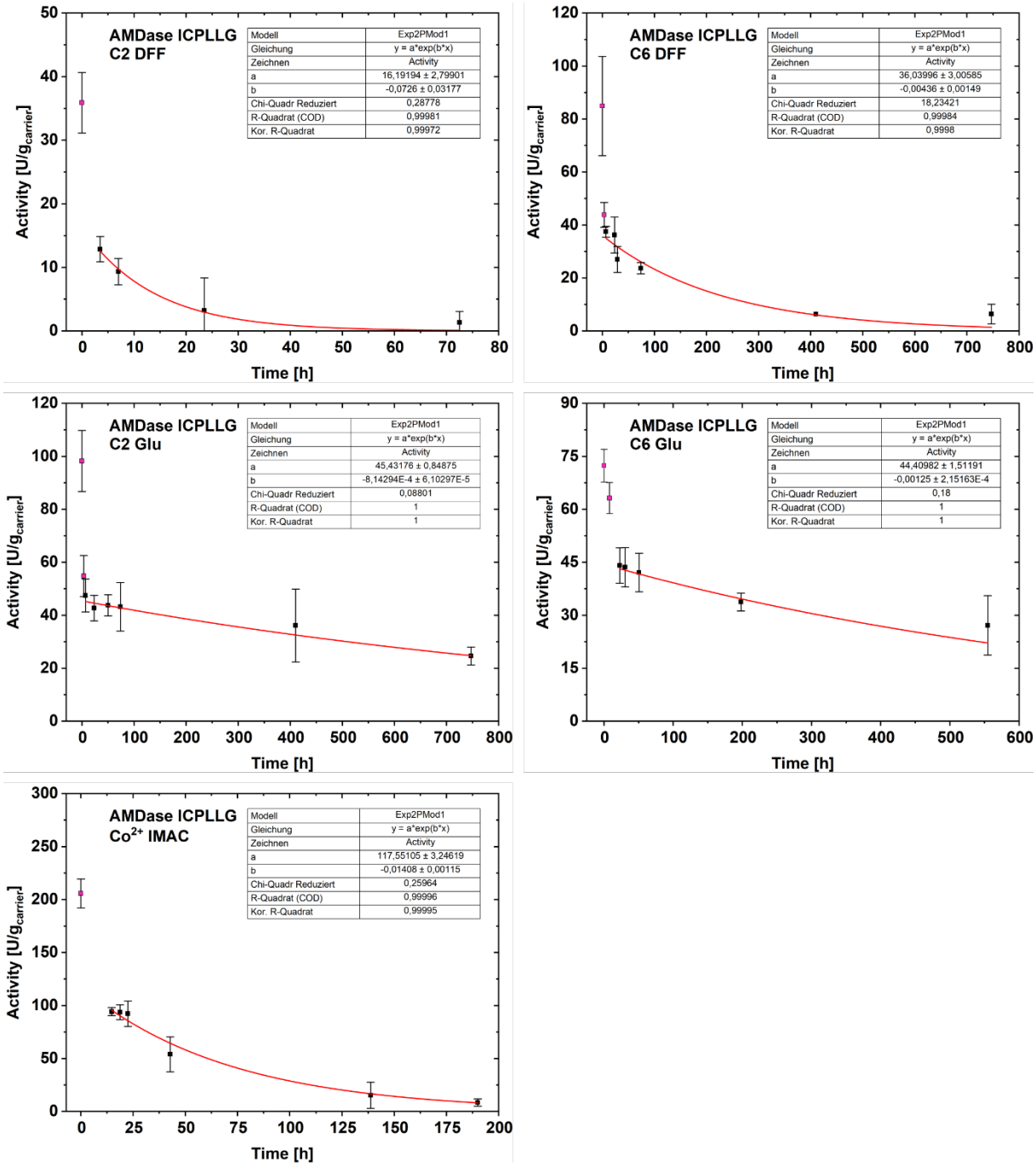

Figure S19. Time-course of the initial mass-specific activities of the AMDase ICPLLG variant immobilized onto different enzyme carriers. The different carriers utilized in this study are specified in **Section 3.3**. Fitting of data points was carried out in Origin with an exponential decay function. Initial data-points (highlighted in pink) show profound enzyme deactivation were excluded. Immobilization was carried out in triplicates (188–291 $mg_{CFE,p}/g_{carrier}$), protein was quantified via BCA-assay. The initial activity of the carrier preparation was determined according to **Section 3.4**. Technical triplicates; 1 mL PMA-reaction-buffer (20mM phenylmalonic acid (**6b**), 50 mM HEPES, pH 7.8); 5 $mg_{carrier}$; 950 rpm, 30°C, 4.25 min total assay time, sampled each minute.

3.6 Saponification

The saponification reaction of dimethyl naproxenmalonate (**1a**) and dimethyl flurbiprofenmalonate (**2a**) resulted in a suspension of the respective disodium malonate. Full conversion was indicated by TLC after 16 hours of reaction time. We investigated the potential addition of the disodium malonate with the

removal of the organic solvent by centrifugation. Reaction mixtures of both malonates (**1b** and **2b**) resulted in the separation into three phases. HPLC analysis of the phases identified the solid disodium flurbiprofenmalonate or disodium naproxenmalonate as precipitate (**Figure S20,** 1), while the reaction products were absent in the organic solvent supernatant (**Figure S20,** 2). However, a third phase (**Figure S20,** 3), with lowest density, could be identified with the deprotected malonates. In reference to literature, this phase observation is the saturated reaction product resulted by liquid-liquid phase separation (LLPS), from which crystal nucleation takes place. Similar "*oiling out*" phenomena have been characterized for the NSAID ibuprofen in aqueous environments and various APIs in solvent mixtures, where a kinetically stabilized liquid precursor phase forms prior to or alongside crystallization.[74,75] We decided not to further investigate process implementations of the precipitate but dissolved the deprotected malonate in water with simultaneous removal of the organic solvent by reduced pressure.

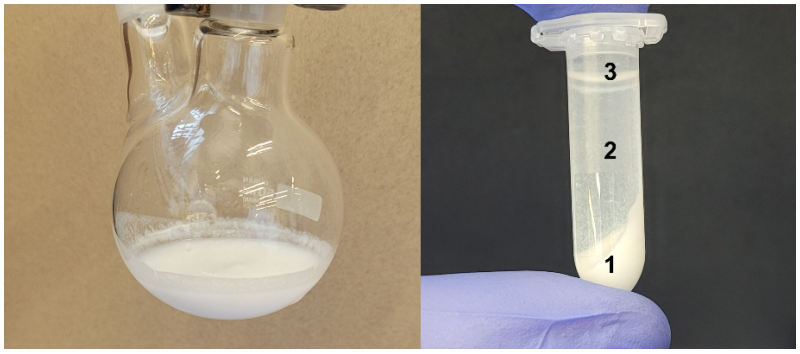

Figure S20. Pictures of the suspension resulted by the saponification of dimethyl flurbiprofenmalonate. Left: Two-neck flask of the reaction mixture after 16 hours. Right: Centrifuged sample of the reaction mixture, which shows three phases. **1**: disodium flurbiprofenmalonate (solid phase), **2**: organic solvent phase of dichloromethane/methanol (liquid phase), **3**: flurbiprofen saturated phase (liquid phase). The different phases were analyzed by HPLC-DAD.

3.7 Rotating bed reactor (RBR)

The biocatalytic synthesis of arylpropionic acid derivates **1c**–**3c** and alkyl-butenoic acids **4c** and **5c** was carried out in a SpinChem® RBR S2. For this, the RBR was assembled according to the manufacturer manual, except the inner filter mesh. This allows the automatic uptake utilizing the forced convection through the RBR, and carrier particles can be added directly to the reaction vessel, without manually packing the reactor. The RBR was equipped with a pH and temperature sensor. Also, a substrate addition port, connected to a syringe pump, a sampling port and a port for the addition of HCl (5 M) were attached to the RBR (**Figure S21**). The temperature was controlled with a thermostat (10 °C–40 °C). The addition of HCl was automated for the first set of experiments and later done manually, without increase of reaction parameter fluctuations or other negative impact.[a] For the automation of pH adjustment a volumetric titrator with the software Titrisoft 3.3.1 was utilized. A pH stat method used with a setpoint of the desired pH. The reactor was filled with 160 mL of buffer (preparative scale reactions: 50 mM HEPES, pH 8.1, or conditions according to **Table S10** of the BO study) The immobilized enzyme was added directly into the buffer. After addition of the immobilized enzyme, the rotating bed reactor was operated at 500 rpm and the immobilized enzyme was drawn into the basket. The addition of

substrate was performed with a syringe pump (for experiments with automated pH compensation: 0.5 mL/min, and with manual pH adjustment: 3 mL/min). Samples (0.2 mL) were taken through the sampling port with a syringe at various time points and terminated in ACN / H_2O (9:1, 200 µL). Concentrations were determined via HPLC as described in **Section 2.1** until >99% conversion was observed. The reaction mixture was drained from the RBR vessel into a beaker, while the RBR was continued to spin. The centrifugal force further drained the loaded reactor bed from residual reaction mixture. The *ee* was determined via gas chiral chromatography **Section 2.3**. Depending on the utilized substrate a different procedure for product isolation was carried out.

For the isolation of naproxen (**1c**) and flurbiprofen (**2c**) the collected reaction mixture was acidified with HCl (5 M, 15 mL) and the solution was altered at 4 °C for 3 h. The precipitated product was filtered and dried under reduced pressure until final characterization.

For the isolation of 2-phenyl propionic acid (**3c**) and 2-alkyl-but-3-enoic acids **4c** and **5c** the collected reaction mixture was acidified with HCl (5 M, 15 mL) and the product extracted with isopropyl acetate (3 x 20 mL). The combined organic phases were washed with brine (20 mL) and dried over $MgSO_4$ and the organic solvent was removed under reduced pressure at 22 °C. Prior characterization 2-alkyl-butenoic acids **4c** and **5c** were purified by flash column chromatography (Cyclohexane:Ethylacetate, 99:1 → 90:10).

[a] Disclosure on manual pH adjustment: Due to a power failure in the building, the volumetric titrator ceased to function. This necessitated manual pH adjustment using a syringe for further experiments. To accomplish this, the pH electrode utilized was connected to a usual pH-meter. Manual adjustment did not cause any significant fluctuation in the experimental parameters; rather, it reduced them. However, the amount of work required at the beginning of the preparative experiments increased significantly.

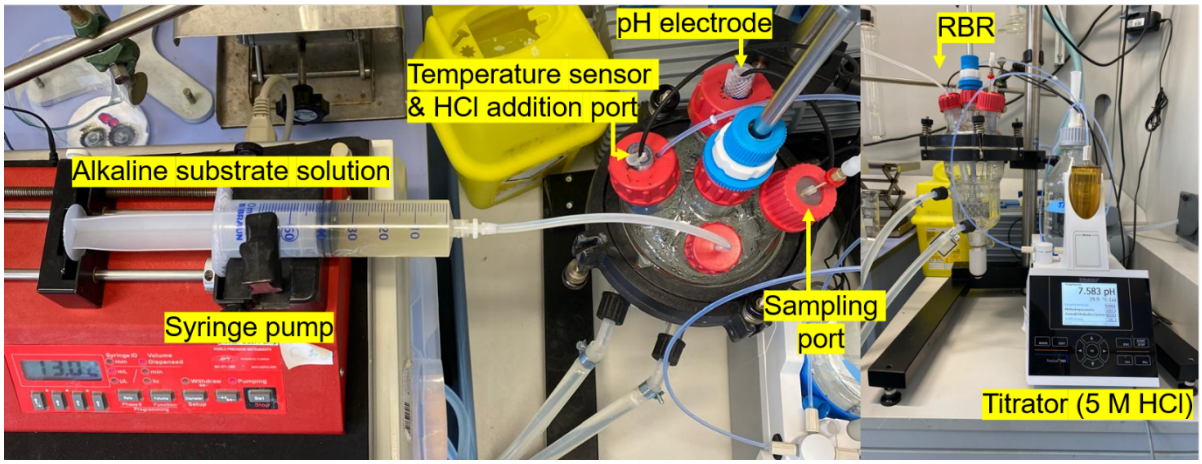

Figure S21. Set-up of the rotating bed rotator (RBR).

3.8 Preparative scale reactions

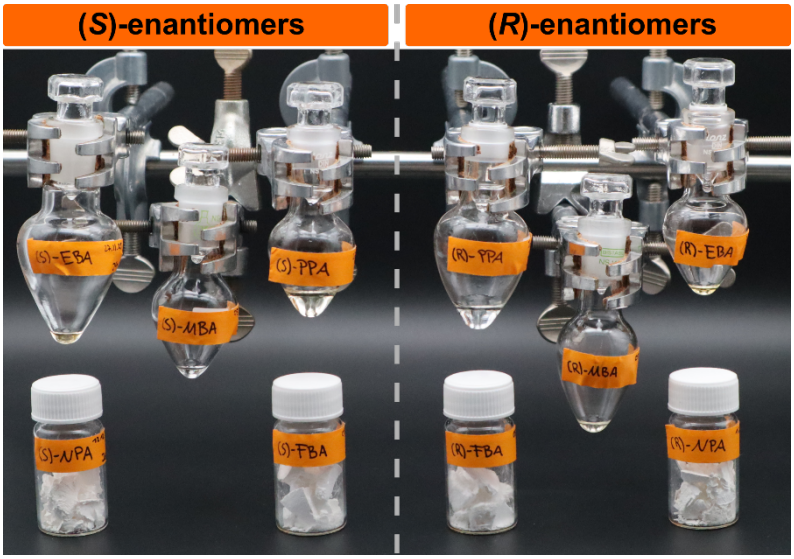

Figure S22. Compilation of all isolated products synthesized in the preparative scale experiments. On the left side are all the (*S*)-enantiomers, and on the right all (*R*)-enantiomers. Abbreviations: NPA: naproxen (**1c**), FBA: flurbiprofen (**2c**), 2-phenyl propionic acid (**3c**), MBA: 2-methyl butenoic acid (**4c**), EBA: 2-ethyl butenoic acid (**5c**).

The process mass intensity (PMI) was calculated based on **equation (S15)**. However, in previously reported works, not all used resources were quantified. To result in a clear undistorted comparison between the different approaches, we decided to neglect the drying agent ($MgSO_4$ or Na_2SO_4) from the calculations.

$$PMI = \frac{mass\ of\ all\ resources}{mass\ of\ product} \tag{S15}$$

For the Global Warming Potential (GWP) analysis[60] we evaluated the biocatalytic production of naproxen with the subsequent downstream as an example. We accounted for treatment of all solvents utilized in the biocatalytic step (reaction buffer, substrate addition and HCl for pH compensation and acidification for product precipitation). The GWP of waste water treatment was calculated based on **equation (S16)** with a pre-treatment factor of f = 0.35, with the product titer $[P]$ = 11.92 g/L of our biocatalytic production of (*S*)-naproxen. The required upstream energy investment was calculated based on **equation (S16)** with the temperature difference ΔT of room top reaction temperature and the reaction time t of our process example of 48 h.

$$\mathrm{GWP(media\ treatment)} = \frac{f}{[P]} \tag{S16}$$

$$\mathrm{GWP\big(water(energy)\big)} = \left(\frac{0.00037 \cdot \Delta T}{[P]}\right) + t \cdot \left(\frac{0.000056 \cdot \Delta T}{[P]}\right) \tag{S17}$$

3.8.1 Product identification by NMR spectroscopy

The quality of NMR spectra did not differ between both enantiomers, which were produced in the intensified process.

Naproxen (**1c**)

^{1}H-NMR (400 MHz, DMSO-d6): δ(ppm)= 7.79 (dd, J = 10.0, 8.8 Hz, 2H), 7.72 (d, J = 1.8 Hz, 1H), 7.41 (dd, J = 8.5, 1.8 Hz, 1H), 7.29 (d, J = 2.6 Hz, 1H), 7.16 (dd, J = 8.9, 2.6 Hz, 1H), 3.87 (s, 3H), 3.81 (q, J = 7.1 Hz, 1H), 1.45 (d, J = 7.1 Hz, 3H).

^{13}C-NMR (101 MHz, DMSO-d6): δ(ppm)= 175.94, 157.59, 136.79, 133.71, 129.58, 128.88, 127.31, 126.88, 126.04, 119.16, 106.17, 55.62, 45.05, 18.91.

Flurbiprofen (**2c**)

^{1}H-NMR (400 MHz, DMSO-d6): δ(ppm)= 12.48 (s, 1H), 7.58 – 7.44 (m, 5H), 7.44 – 7.36 (m, 1H), 7.28 – 7.20 (m, 2H), 3.78 (q, J = 7.1 Hz, 1H), 1.42 (d, J = 7.2 Hz, 3H).

^{13}C-NMR (101 MHz, DMSO-d6): δ(ppm)= 175.35, 159.34 (d, J(C-F) = 245.9 Hz), 143.59 (d, J(C-F) = 7.7 Hz), 135.38, 131.15 (d, J(C-F) = 3.9 Hz), 130.17 – 128.13 (m), 128.25, 127.11 (d, J(C-F) = 13.3 Hz), 124.50 (d, J(C-F) = 3.1 Hz), 115.62 (d, J(C-F) = 23.3 Hz), 44.57, 18.75.

2-Phenylpropionic acid (**3c**)

^{1}H-NMR (400 MHz, $CDCl_3$): δ(ppm)= 7.40 – 7.34 (m, 5H), 7.35 – 7.29 (m, 1H), 7.32 – 7.26 (m, 1H), 3.77 (q, J = 7.2 Hz, 1H), 1.55 (d, J = 7.2 Hz, 3H).

^{13}C-NMR (101 MHz, $CDCl_3$): δ(ppm)= 180.70, 139.75, 128.71, 127.62, 127.42, 45.36, 18.12.

2-Methylbut-3-enoic acid (**4c**)

^{1}H-NMR (400 MHz, $CDCl_3$): δ(ppm)= 5.94 (ddd, J = 17.5, 10.3, 7.4 Hz, 1H), 5.24 – 5.11 (m, 2H), 3.19 (pt, J = 7.1, 1.2 Hz, 1H), 1.31 (d, J = 7.1 Hz, 3H).

^{13}C-NMR (101 MHz, $CDCl_3$): δ(ppm)= 179.86, 136.43, 116.51, 43.32, 16.50.

2-Ethylbut-3-enoic acid (**5c**)

^{1}H-NMR (400 MHz, $CDCl_3$): δ(ppm)= 5.84 (ddd, J = 17.3, 9.9, 8.6 Hz, 1H), 5.25 – 5.16 (m, 2H), 3.02 – 2.92 (m, 1H), 1.93 – 1.78 (m, 1H), 1.71 – 1.56 (m, 1H), 0.97 (t, J = 7.4 Hz, 3H).

^{13}C-NMR (101 MHz, $CDCl_3$): δ(ppm)= 180.00, 135.27, 117.81, 51.59, 25.22, 11.51.

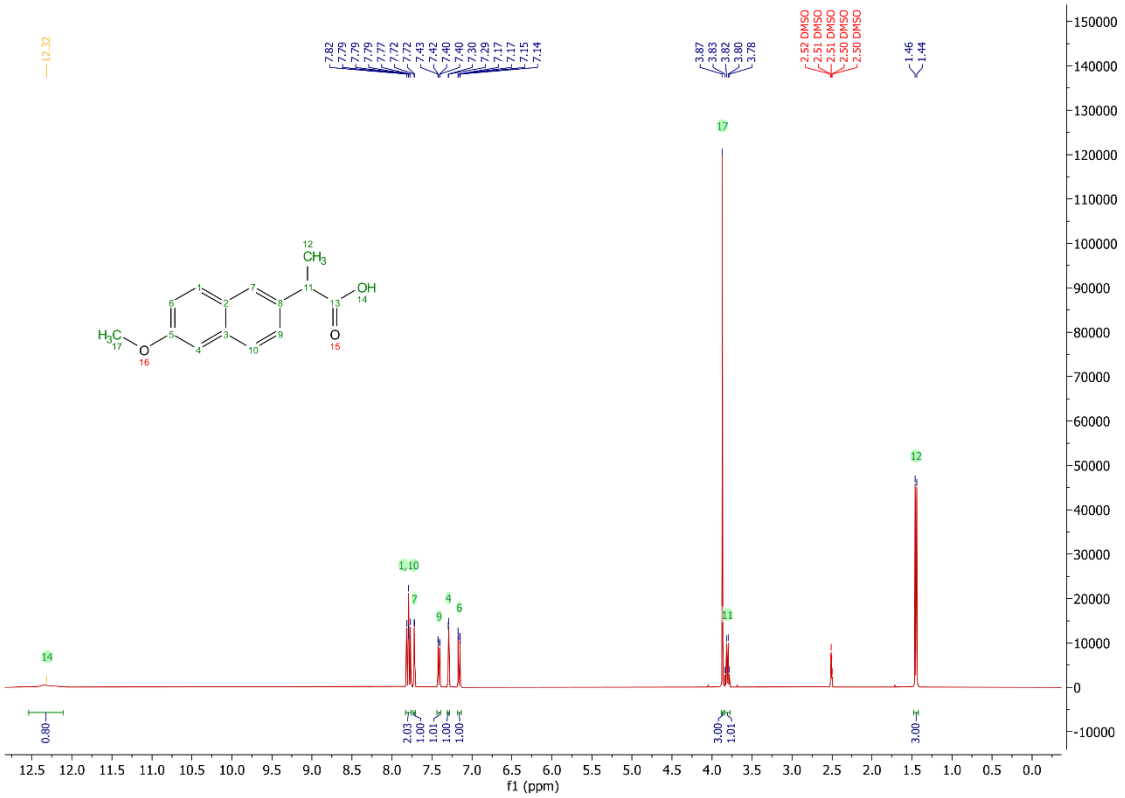

Figure S23. Measured ^{1}H-NMR spectrum of naproxen (**1c**) in DMSO-d6, produced with the intensified process.

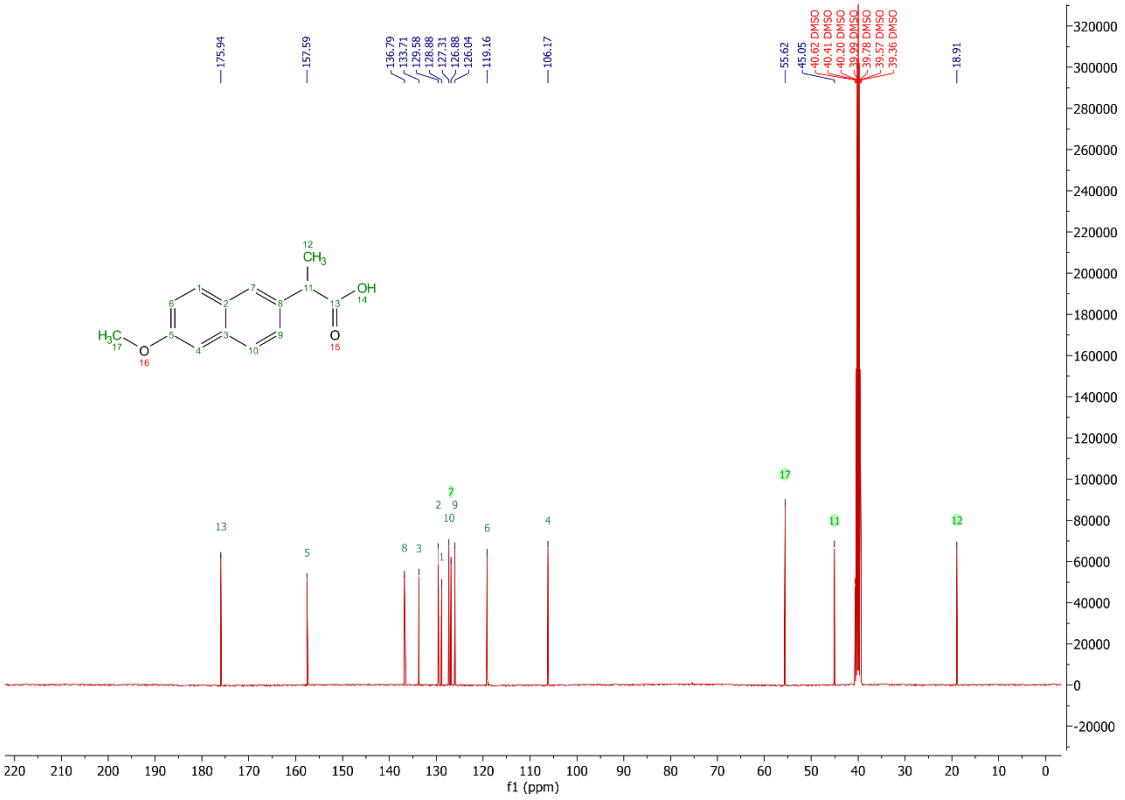

Figure S24. Measured ^{13}C-NMR spectrum of naproxen (**1c**) in DMSO-d6, produced with the intensified process.

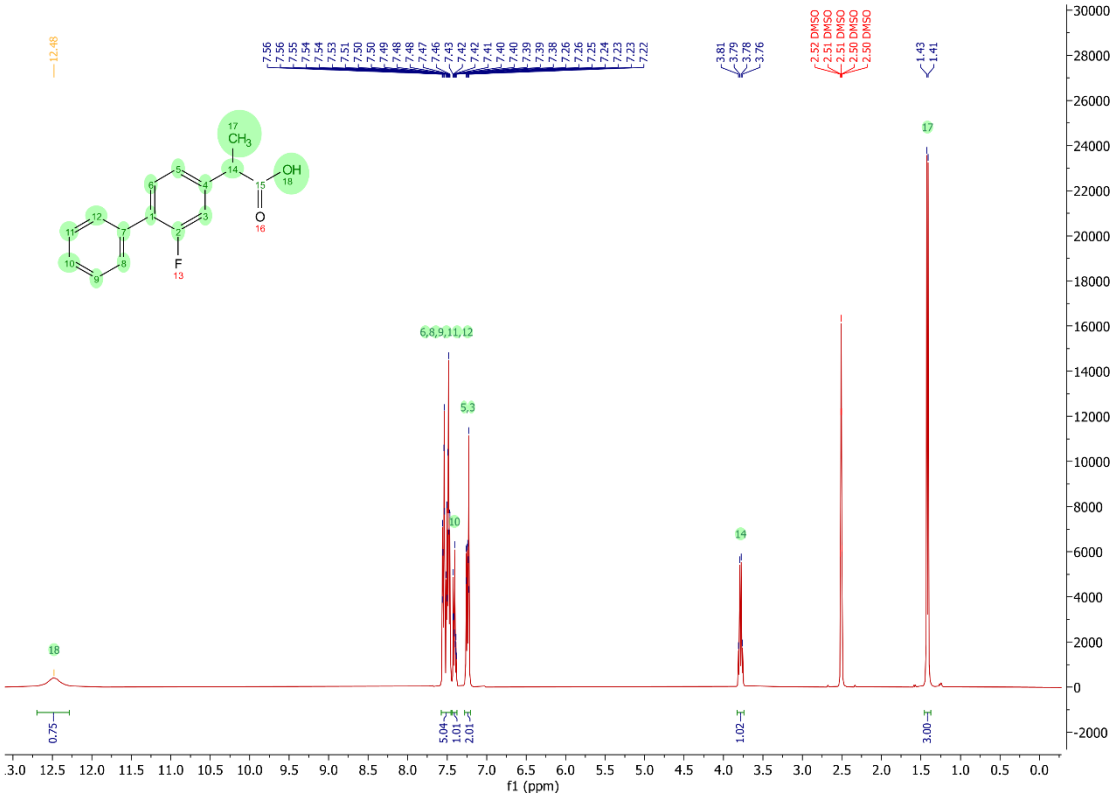

Figure S25. Measured ^{1}H-NMR spectrum of flurbiprofen (**2c**) in DMSO-d6, produced with the intensified process.

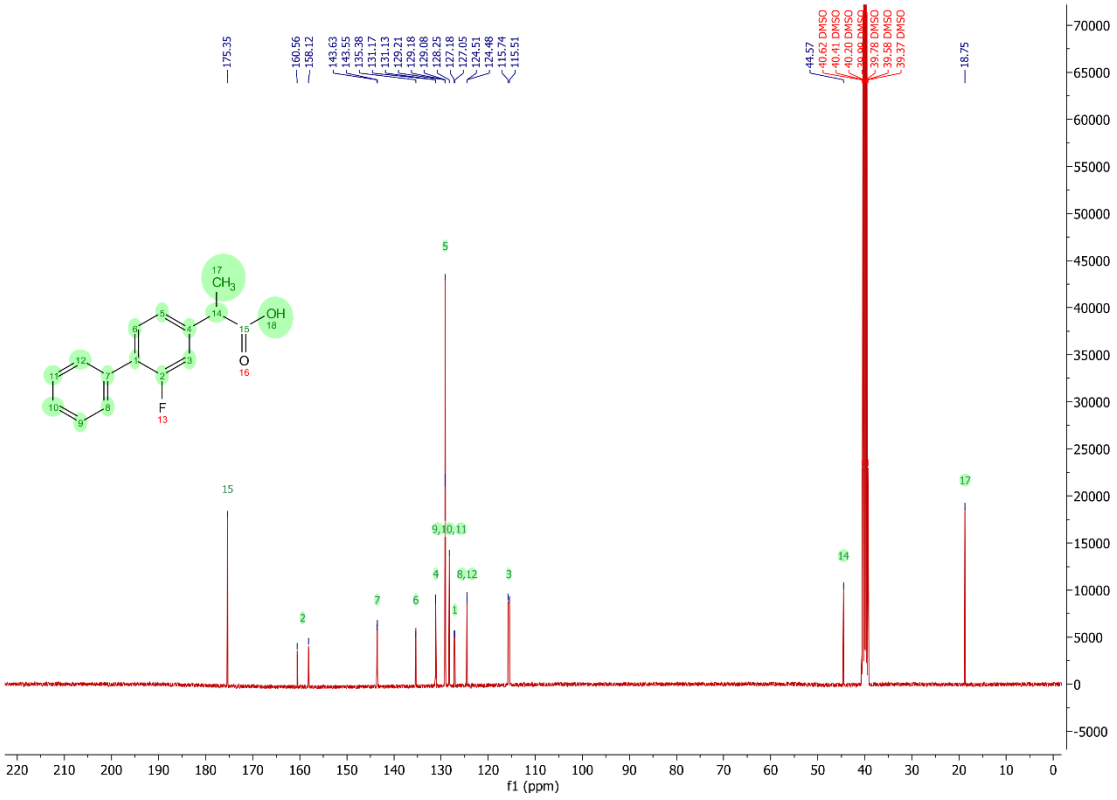

Figure S26. Measured ^{13}C-NMR spectrum of flurbiprofen (**2c**) in DMSO-d6, produced with the intensified process.

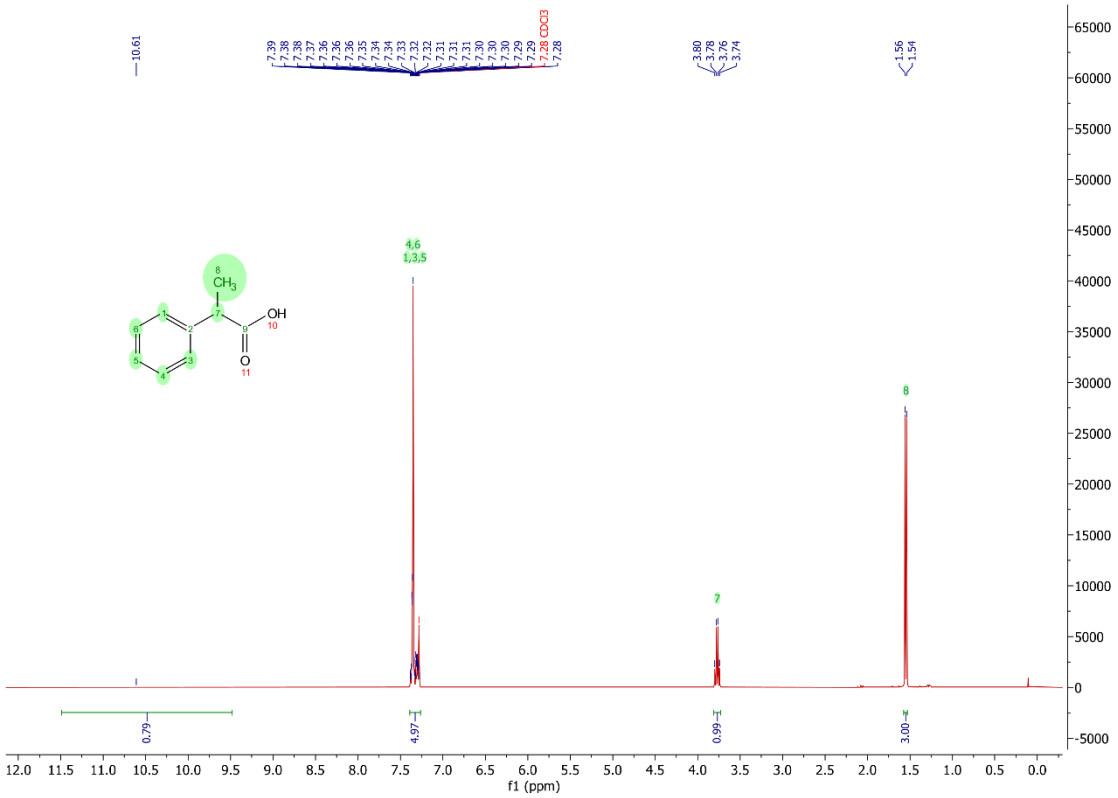

Figure S27. Measured ^{1}H-NMR spectrum of 2-phenylpropionic acid (**3c**) in $CDCl_3$, produced with the intensified process

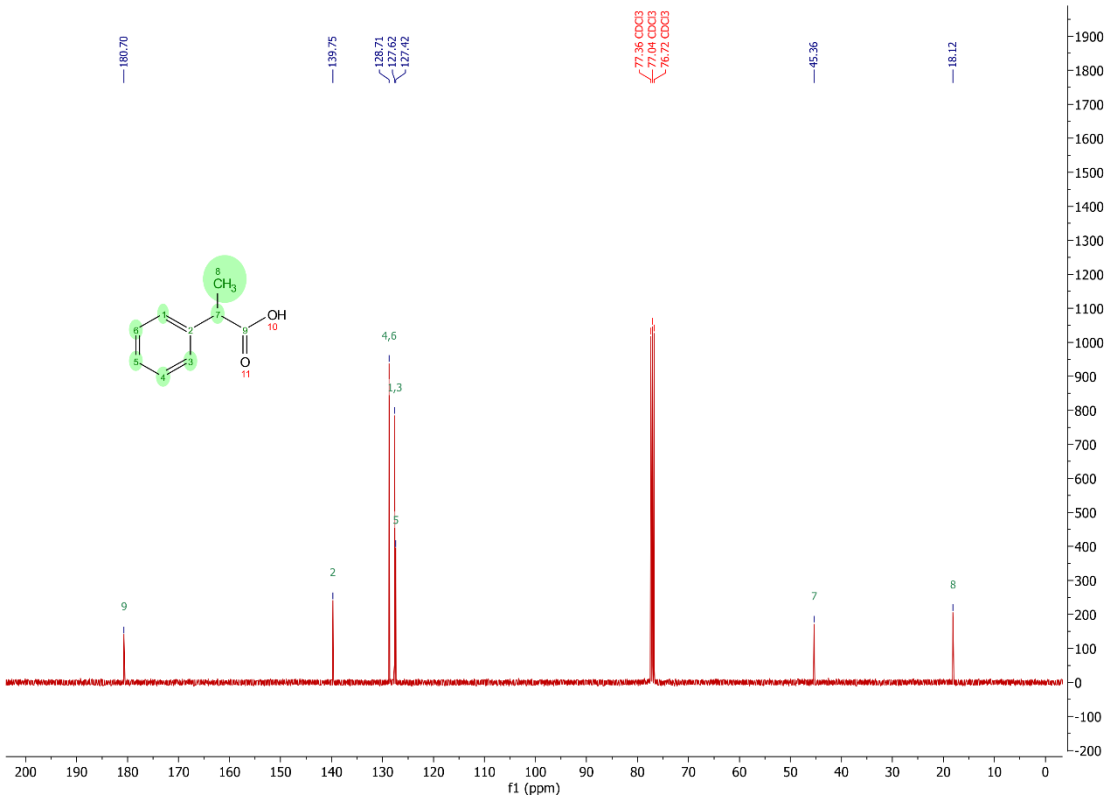

Figure S28. Measured ^{13}C-NMR spectrum of 2-phenylpropionic acid (**3c**) in $CDCl_3$, produced with the intensified process.

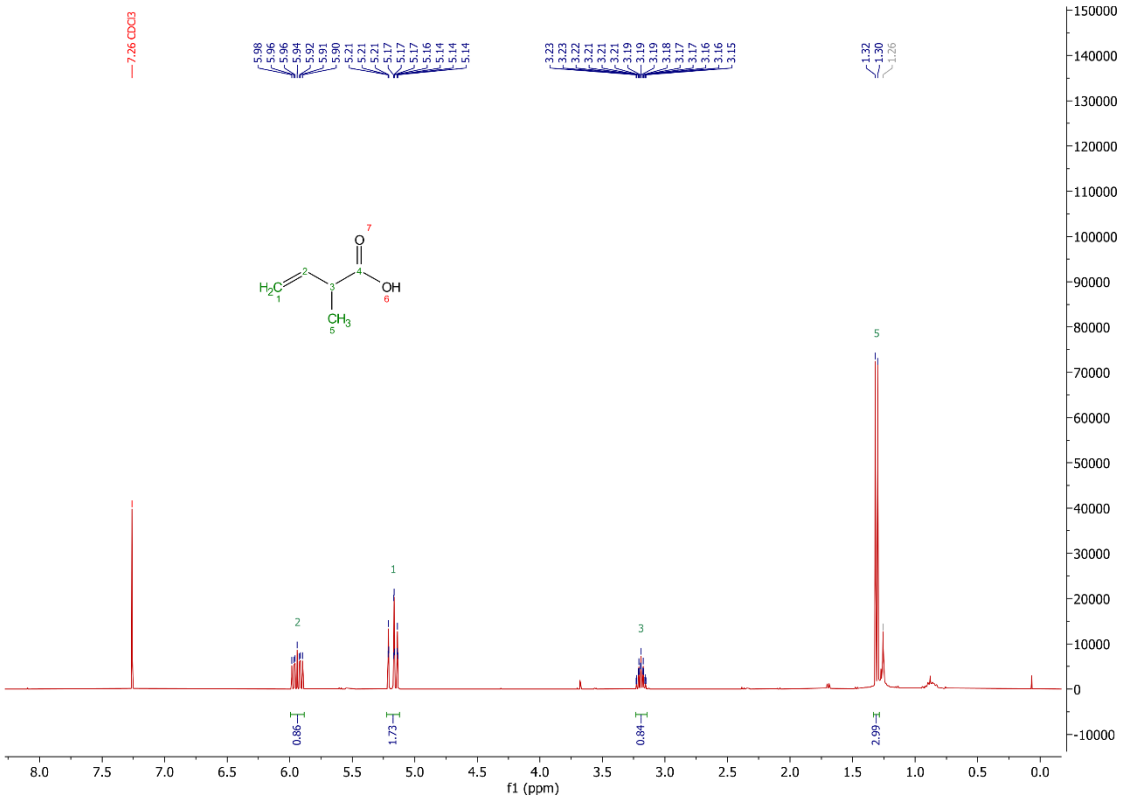

Figure S29. Measured ^{1}H-NMR spectrum of 2-methylbut-3-enoic acid (**4c**) in $CDCl_3$, produced with the intensified process.

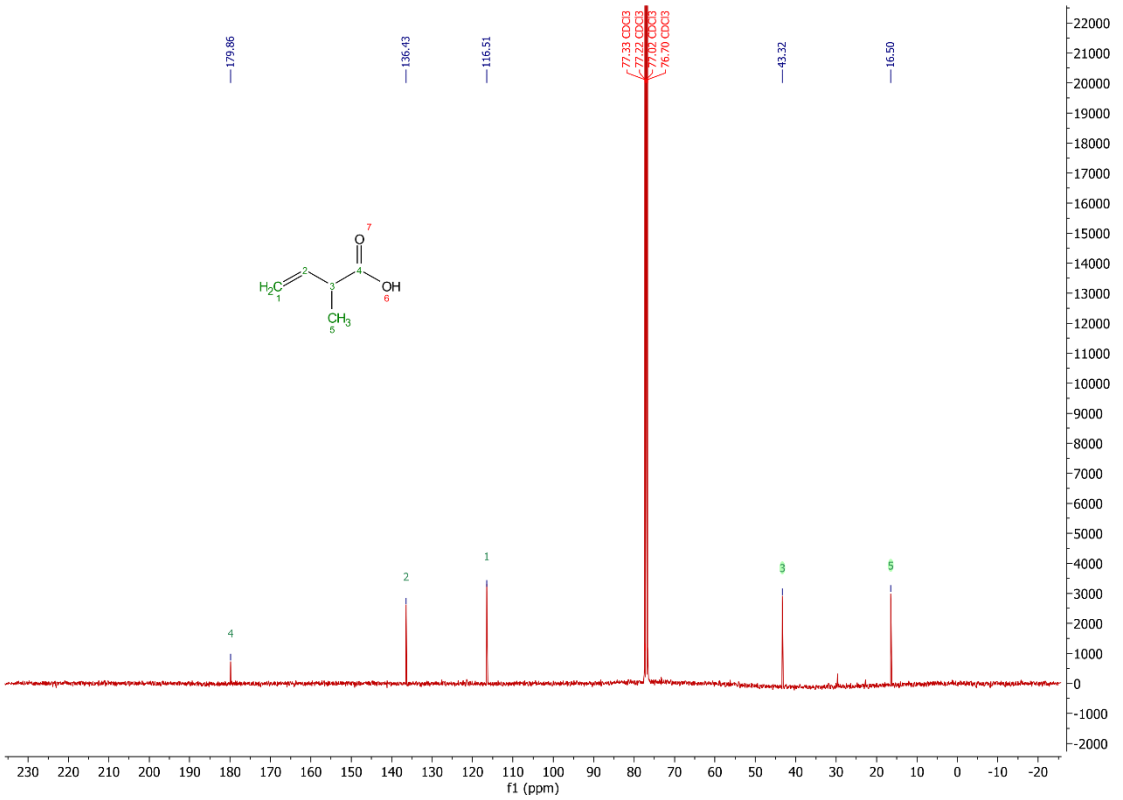

Figure S30. Measured ^{13}C-NMR spectrum of 2-methylbut-3-enoic acid (**4c**) in $CDCl_3$, produced with the intensified process.

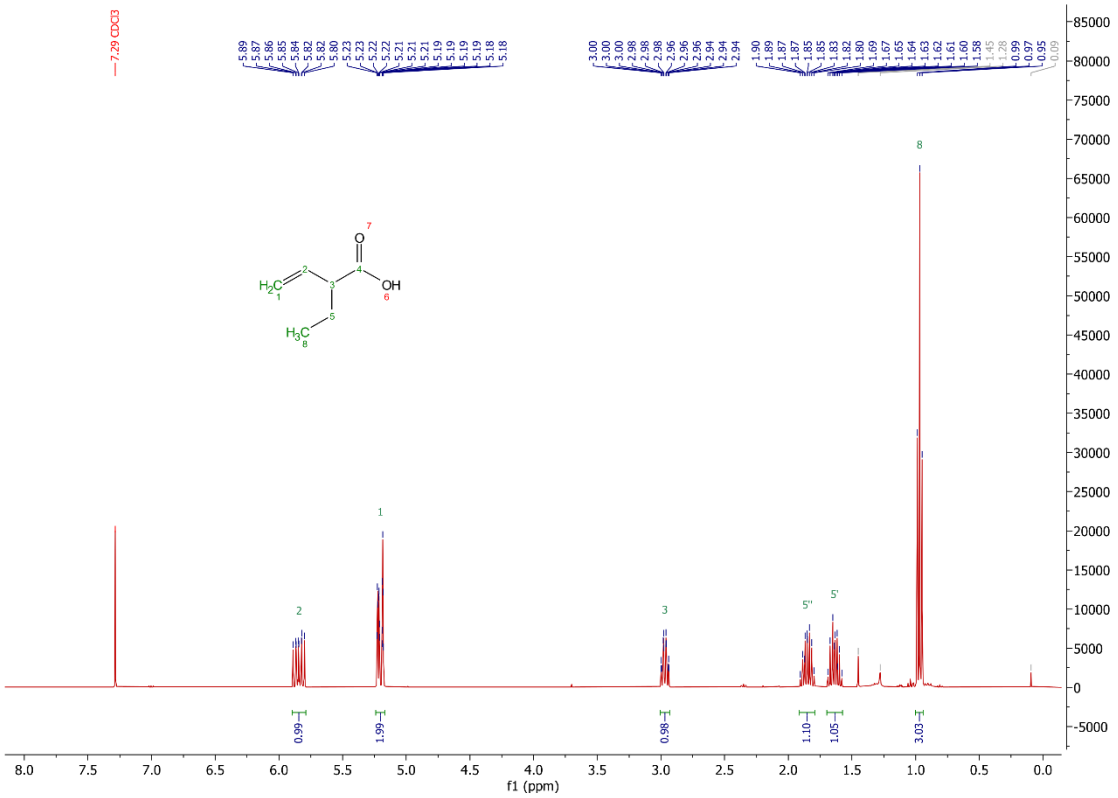

Figure S31. Measured ^{1}H-NMR spectrum of 2-ethylbut-3-enoic acid (**5c**) in $CDCl_3$, produced with the intensified process.

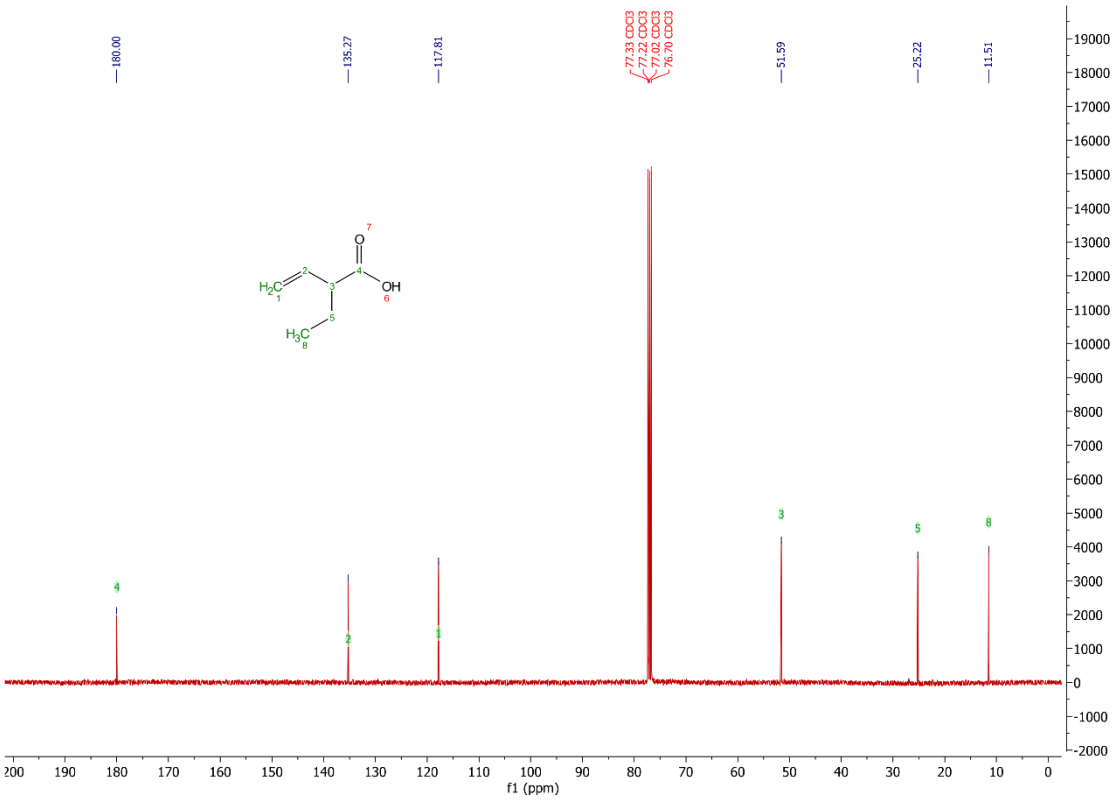

Figure S32. Measured ^{13}C-NMR spectrum of 2-ethylbut-3-enoic acid (**5c**) in $CDCl_3$, produced with the intensified process.

4 Substrate Synthesis

Phenyl malonic acid was purchased from TCI chemicals. 2-alkyl-2-vinyl malonic acids **4b** and **5b** were synthesized according to van der Pol & Gerstenberger *et al*.[36]

Unless indicated, all reactions were carried out under inert atmosphere (Nitrogen or Argon, dried over phosphorus pentoxide). Glassware was stored in a drying cabinet at 60 °C, heated three times under reduced pressure, and flushed with inert gas before use. Syringes and cannulas were flushed three times with inert gas. The temperatures specified refer to the respective oil- or cooling bath temperatures.

4.1 General procedure for the synthesis of methyl 2-(6-methoxynaphthalen-2-yl)propanoate and methyl 2-(2-fluoro-[1,1'-biphenyl]-4-yl)propanoate

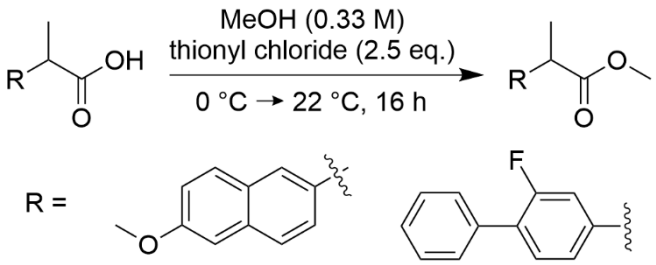

2-(6-methoxynaphthalen-2-yl)propanoic acid (25.00 g, 111.0 mmol, 1.0 eq.) or 2-(2-fluoro-[1,1'-biphenyl]-4-yl)propanoic acid (25.00 g, 102.3 mmol, 1.0 eq.) was dissolved in degassed methanol (333 mL, 0.33 M) and thionyl chloride (2.5 eq.) was added dropwise while stirring (600 rpm) at 0 °C. The reaction mixture was allowed to warm to room temperature over 16 h. The reaction was terminated by the addition of a mixture of water and ice (100 mL) with adjustment to pH 4 with NaOH (10 M). The solvent was concentrated under reduced pressure, with subsequent extraction (EtOAc, 3 x 150 mL). The combined organic phases were washed with brine (200 mL) and dried over $MgSO_4$. The solvent was removed under reduced pressure to receive the product as white solid, which was used without further purification.

TLC: Cyclohexane:Ethylacetate, 1:5.

Recrystallization in ethanol possible.

Methyl 2-(6-methoxynaphthalen-2-yl)propanoate (26.02 g, 106.5 mmol, 98.1%)

^{1}H-NMR (400 MHz, $CDCl_3$): δ(ppm)= 7.71 (d, J = 8.6 Hz, 2H), 7.67 (dt, J = 1.6, 0.8 Hz, 1H), 7.41 (dd, J = 8.5, 1.8 Hz, 1H), 7.17 – 7.10 (m, 2H), 3.91 (s, 3H), 3.86 (q, J = 7.1 Hz, 1H), 3.67 (s, 3H), 1.58 (d, J = 7.1 Hz, 3H).

^{13}C-NMR (101 MHz, $CDCl_3$): δ(ppm)= 175.16, 157.67, 135.69, 133.71, 129.29, 128.95, 127.19, 126.20, 125.95, 119.01, 105.61, 55.32, 52.06, 45.36, 18.61.

Methyl 2-(2-fluoro-[1,1'-biphenyl]-4-yl)propanoate (25.70 g, 99.5 mmol, 97.2%)

^{1}H-NMR (400 MHz, $CDCl_3$): δ(ppm)= 7.56 – 7.51 (m, 2H), 7.47 – 7.33 (m, 5H), 7.17 – 7.13 (m, 2H), 7.11 (d, J = 1.8 Hz, 1H), 3.77 (q, J = 7.2 Hz, 1H), 3.71 (s, 3H), 1.54 (d, J = 7.2 Hz, 3H).

^{13}C-NMR (101 MHz, $CDCl_3$): δ(ppm)= 174.46, 159.70 (d, J(C-F) = 248.5 Hz), 141.81 (d, J(C-F) = 7.6 Hz), 135.51 (d, J(C-F) = 1.2 Hz), 130.84 (d, J(C-F) = 4.0 Hz), 128.96 (d, J(C-F) = 2.8 Hz), 128.45, 127.86 (d, J(C-F) = 13.4 Hz), 127.67, 123.53 (d, J(C-F) = 3.5 Hz), 115.25 (d, J(C-F) = 23.7 Hz), 52.24, 44.93 (d, J(C-F) = 1.8 Hz), 18.45.

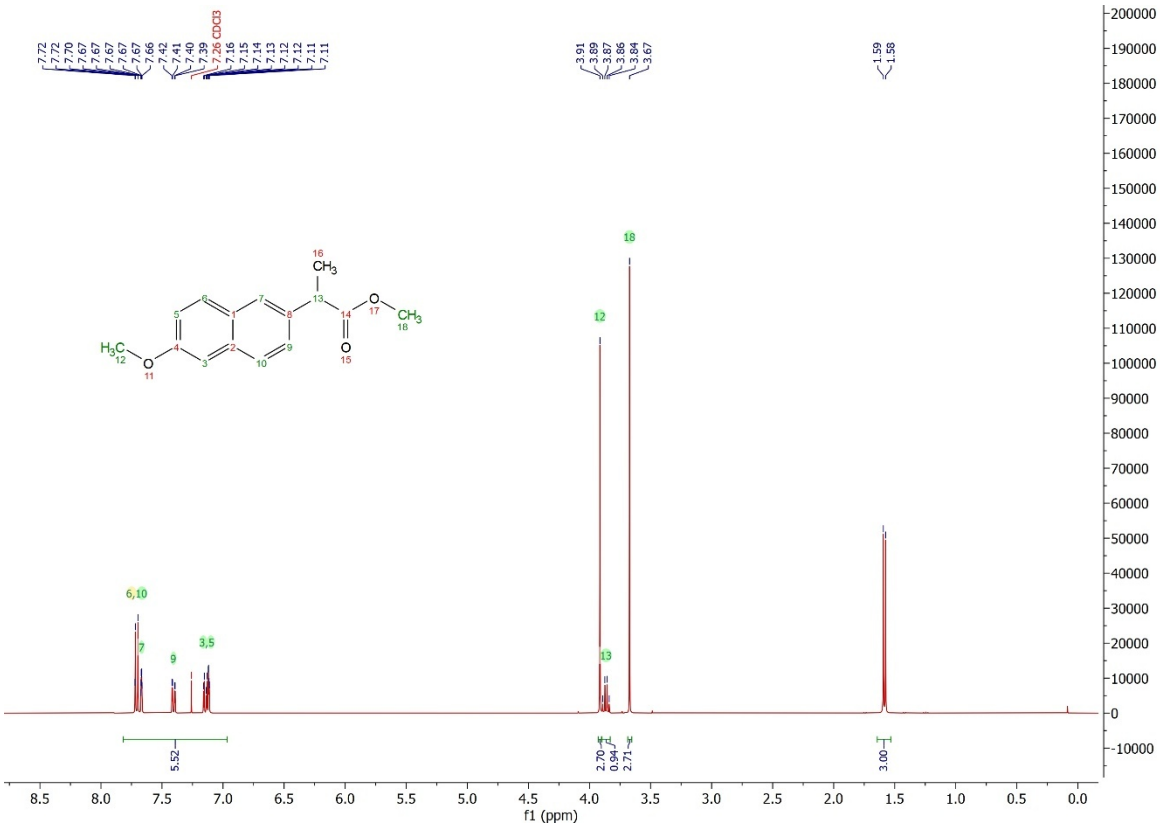

Figure S33. Measured ^{1}H-NMR spectrum of methyl 2-(6-methoxynaphthalen-2-yl)propanoate in $CDCl_3$.

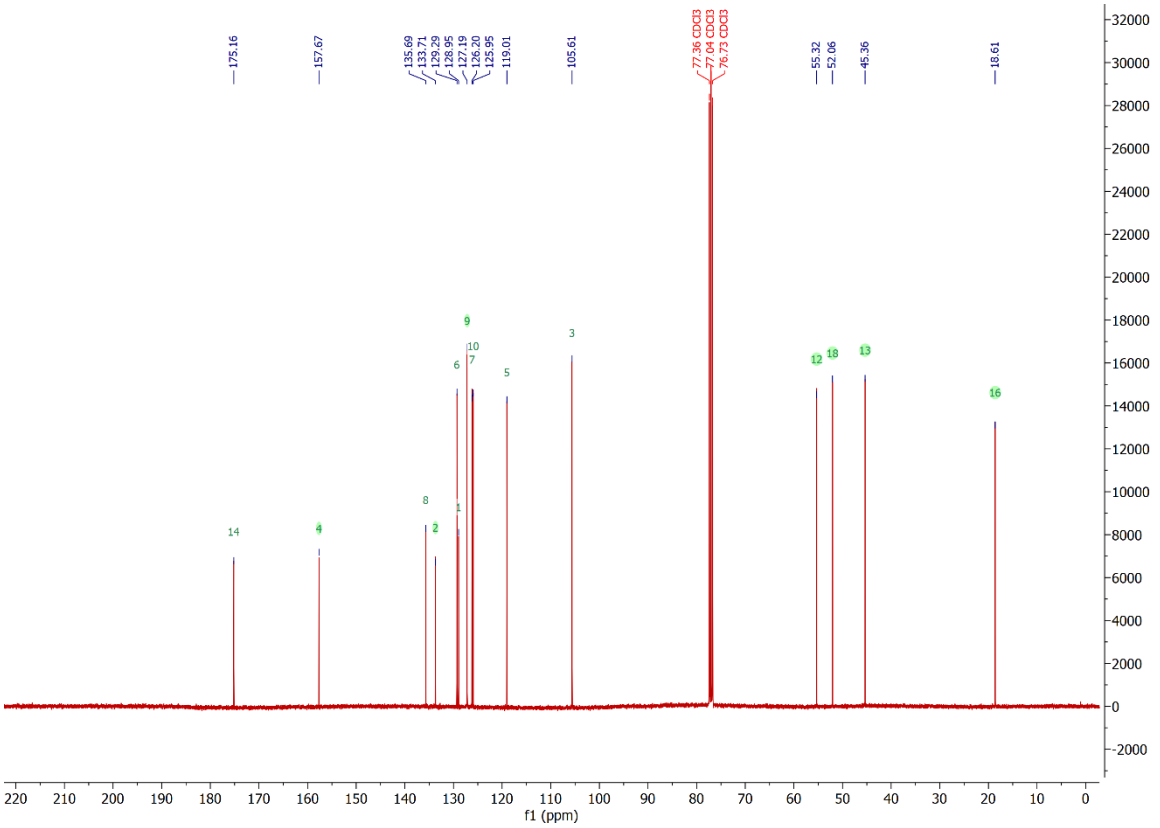

Figure S34. Measured ^{13}C-NMR spectrum of methyl 2-(6-methoxynaphthalen-2-yl)propanoate in $CDCl_3$.

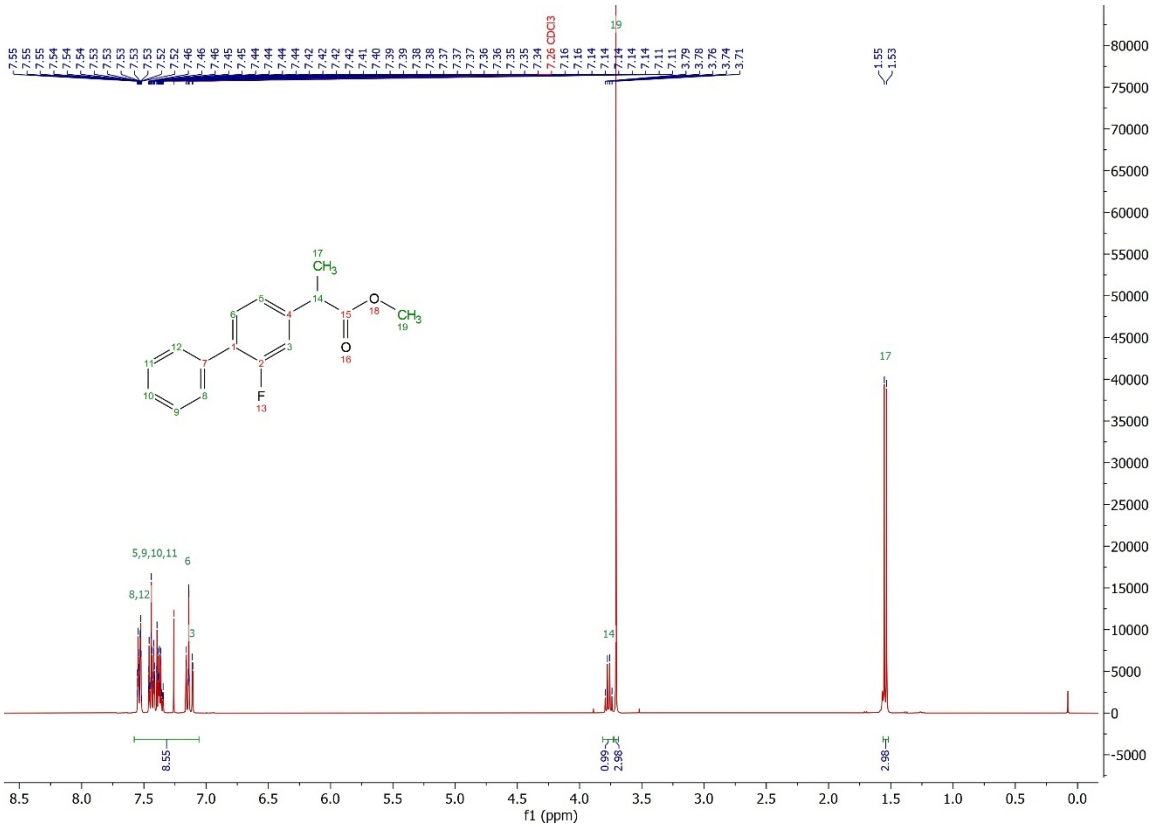

Figure S35. Measured ^{1}H-NMR spectrum of methyl 2-(2-fluoro-[1,1'-biphenyl]-4-yl)propanoate in $CDCl_3$.

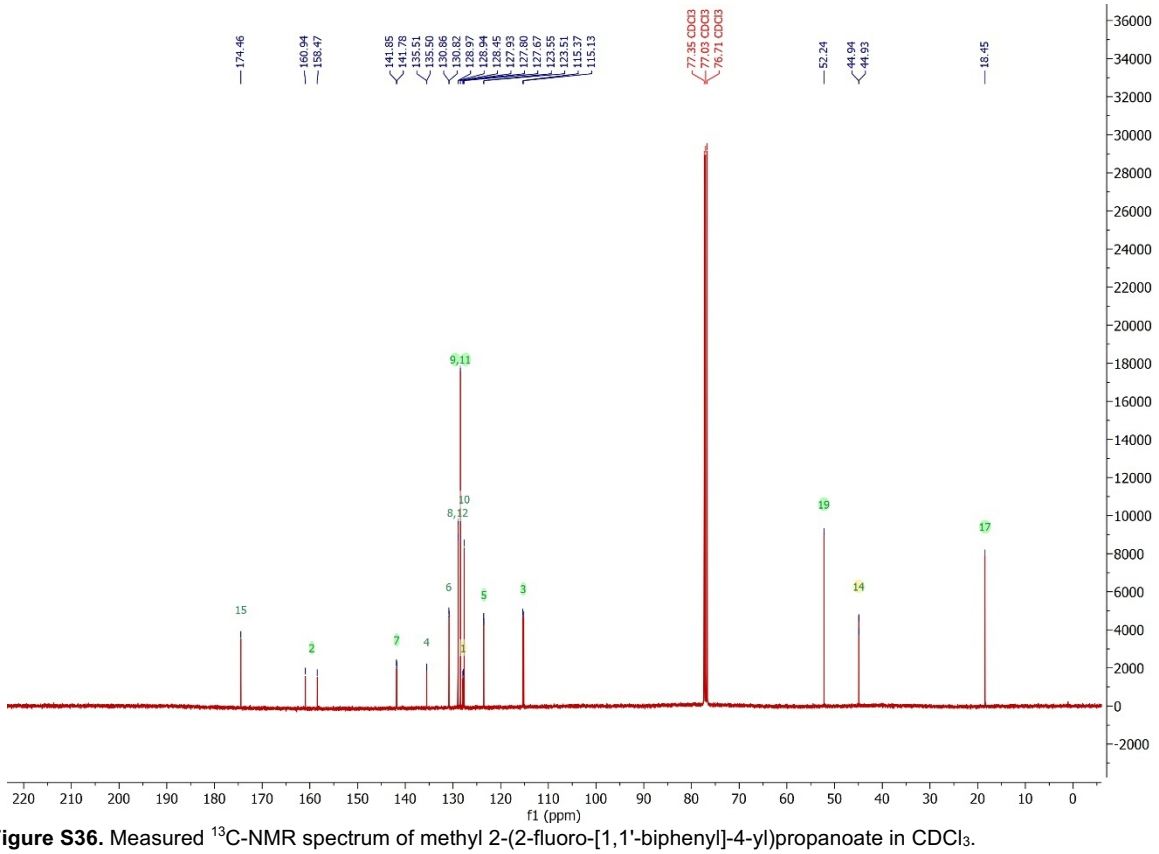

Figure S36. Measured ^{13}C-NMR spectrum of methyl 2-(2-fluoro-[1,1'-biphenyl]-4-yl)propanoate in $CDCl_3$.

4.2 General Procedure for the Synthesis of Dimethyl 2-(6-methoxynaphthalen-2-yl)-2-methylmalonate (1a) and Dimethyl 2-(2-fluoro-[1,1'-biphenyl]-4-yl)-2-methylmalonate (2a)

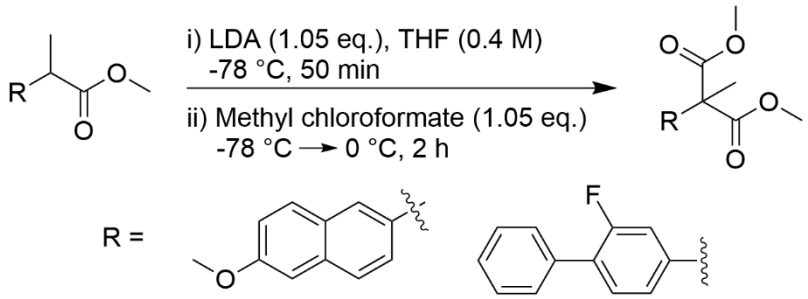

The synthesis of dimethyl naproxenmalonate (**1a**) and dimethyl flurbiprofenmalonate (**2a**) was done according to a modified procedure of Terao *et al.*[76] For this diisopropylamine (1.05 eq.) in dry THF (0.4 M) was cooled to -78 °C and *n*-BuLi in hexane (1.05 eq.) was added dropwise while stirring (600 rpm). The solution was stirred at -78 °C for 1 min and the starting material methyl 2-(6-methoxynaphthalen-2-yl)propanoate (26.02 g, 106.5 mmol) or methyl 2-(2-fluoro-[1,1'-biphenyl]-4-yl)propanoate (25.70 g, 99.5 mmol, 97.2%) dissolved in dry THF (50 mL) was added through a transfer cannula and stirred for another 15 min. Methyl chloroformate (1.05 eq.) was added dropwise and the reaction mixture stirred for 15 min at -78 °C and 2 h at 0 °C. The reaction was terminated with double the volume of a mixture of 1 M NH_4Cl solution mixed with ice and 100 mL EtOAc. Adjustment to pH 5 was done and extracted with EtOAc (3x100 mL). The combined organic phases were washed with brine (100 mL) and dried over anhydrous $MgSO_4$. The solvent was removed under reduced pressure and recrystallized in EtOAc / Cyclohexane (1:9) to receive the product as white solid.

TLC: Cyclohexane:Ethylacetate, 1:5.

Dimethyl 2-(6-methoxynaphthalen-2-yl)-2-methylmalonate (**1a**) (18.48 g, 61.1 mmol, 57.4%)

^{1}H-NMR (400 MHz, $CDCl_3$): δ(ppm)= 7.74 – 7.69 (m, 3H), 7.45 (dd, J = 8.6, 2.1 Hz, 1H), 7.15 (dd, J = 8.8, 2.5 Hz, 1H), 7.12 (d, J = 2.4 Hz, 1H), 3.92 (s, 3H), 3.78 (s, 6H), 1.98 (s, 3H).

^{13}C-NMR (101 MHz, $CDCl_3$): δ(ppm)= 172.20, 158.10, 133.84, 133.26, 129.76, 128.43, 126.70, 126.41, 125.63, 119.02, 105.45, 58.79, 55.34, 52.93, 22.31.

The crystal structure of compound **1a** has been deposited at the Cambridge Crystallographic Data Centre (CCDC) under deposition number 2546401 (DOI: 10.5517/ccdc.csd.cc2rgqzy)

Dimethyl 2-(2-fluoro-[1,1'-biphenyl]-4-yl)-2-methylmalonate (**2a**) (15.78 g, 49.9 mmol, 50.1%)

^{1}H-NMR (400 MHz, $CDCl_3$): δ(ppm)= 7.62 – 7.56 (m, 2H), 7.52 – 7.45 (m, 3H), 7.46 – 7.40 (m, 1H), 7.29 – 7.25 (m, 1H), 7.27 – 7.23 (m, 1H), 3.85 (s, 6H), 1.96 (s, 3H).

^{13}C-NMR (101 MHz, $CDCl_3$): δ(ppm)= 171.54, 159.33 (d, J(C-F) = 247.7 Hz), 139.26 (d, J(C-F) = 7.7 Hz), 135.25 (d, J(C-F) = 1.4 Hz), 130.40 (d, J(C-F) = 4.1 Hz), 130.45 – 126.91 (m), 128.50, 128.48, 127.83, 123.39 (d, J(C-F) = 3.3 Hz), 115.62 (d, J(C-F) = 25.2 Hz), 58.41 (d, J(C-F) = 1.6 Hz), 53.11, 22.23.

The crystal structure of compound **2a** has been deposited at the Cambridge Crystallographic Data Centre (CCDC) under deposition number 2546399 (DOI: 10.5517/ccdc.csd.cc2rgqxw).

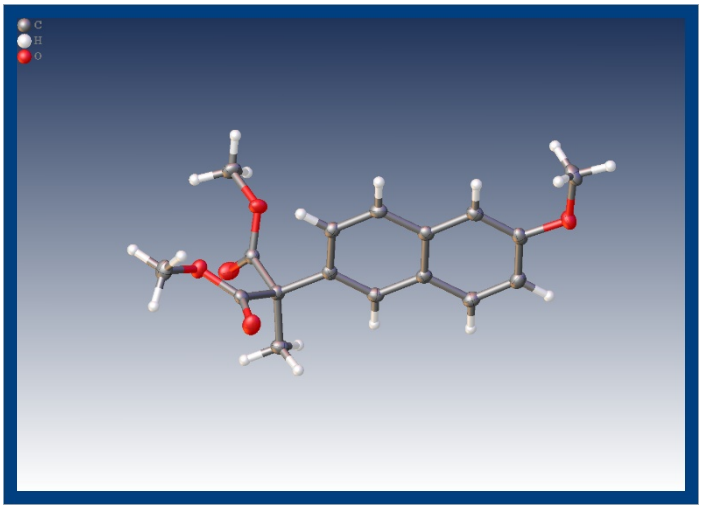

Figure S37. Determined crystal structure of dimethyl 2-(6-methoxynaphthalen-2-yl)-2-methylmalonate (**1a**) (deposition number: 2546401, DOI: 10.5517/ccdc.csd.cc2rgqzy).

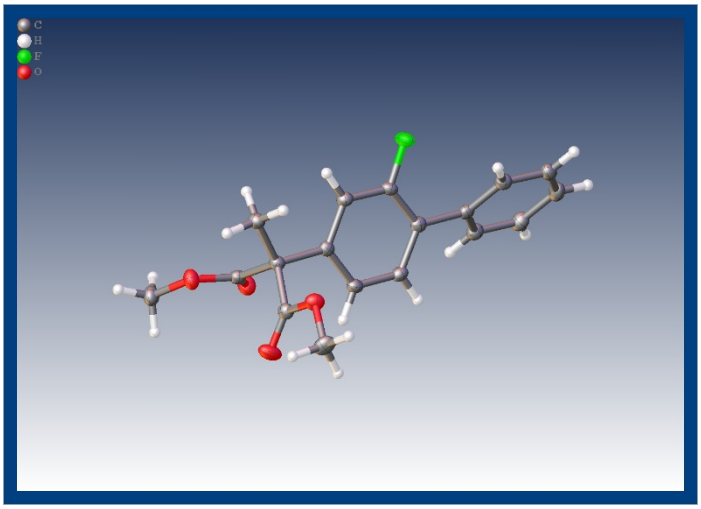

Figure S38. Determined crystal structure of dimethyl 2-(6-methoxynaphthalen-2-yl)-2-methylmalonate (**1a**) (deposition number: 2546399, DOI: 10.5517/ccdc.csd.cc2rgqxw).

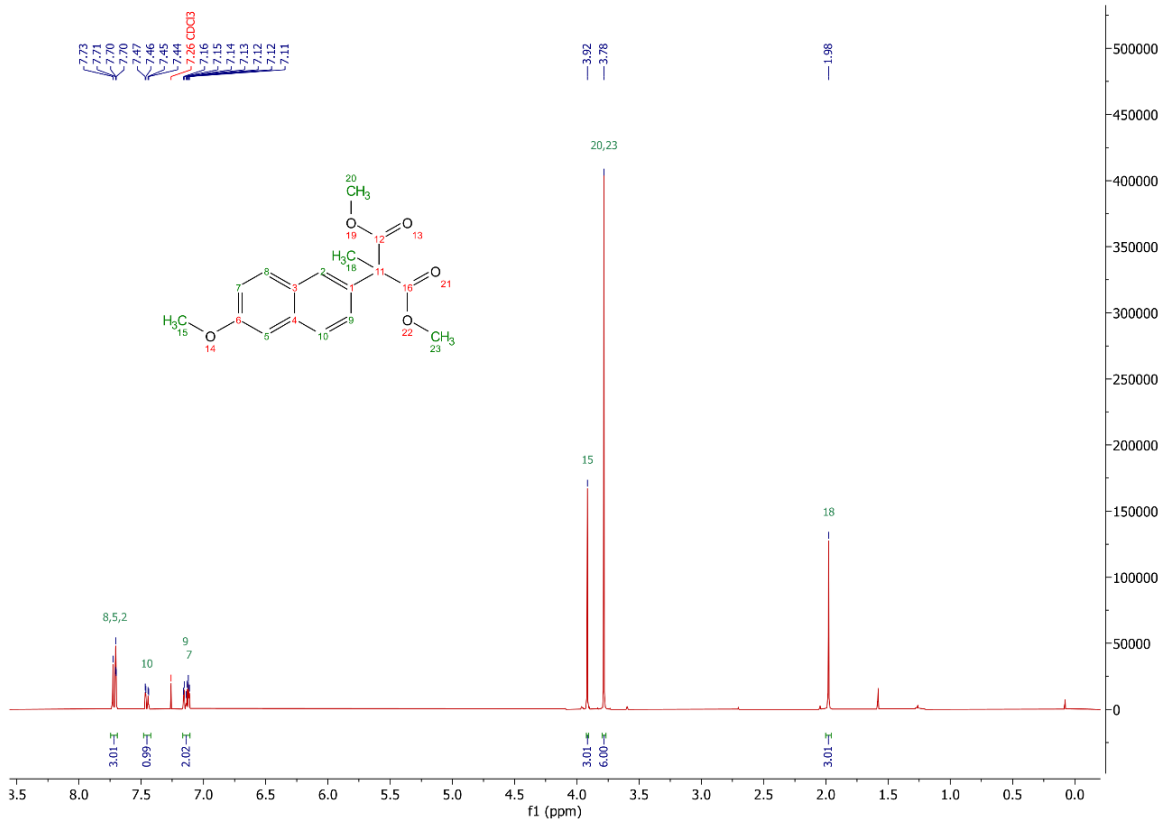

Figure S39. Measured ^{1}H-NMR spectrum of dimethyl 2-(6-methoxynaphthalen-2-yl)-2-methylmalonate (**1a**) in $CDCl_3$.

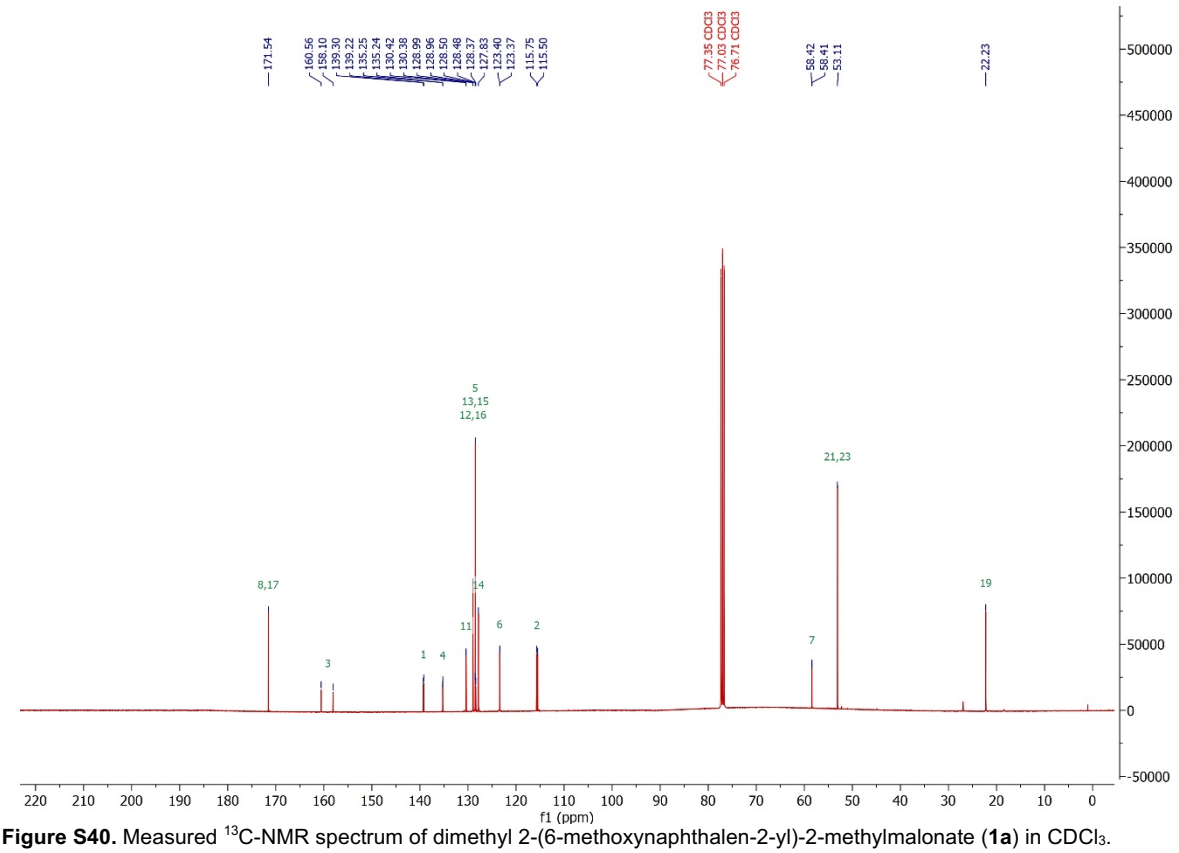

Figure S40. Measured ^{13}C-NMR spectrum of dimethyl 2-(6-methoxynaphthalen-2-yl)-2-methylmalonate (**1a**) in $CDCl_3$.

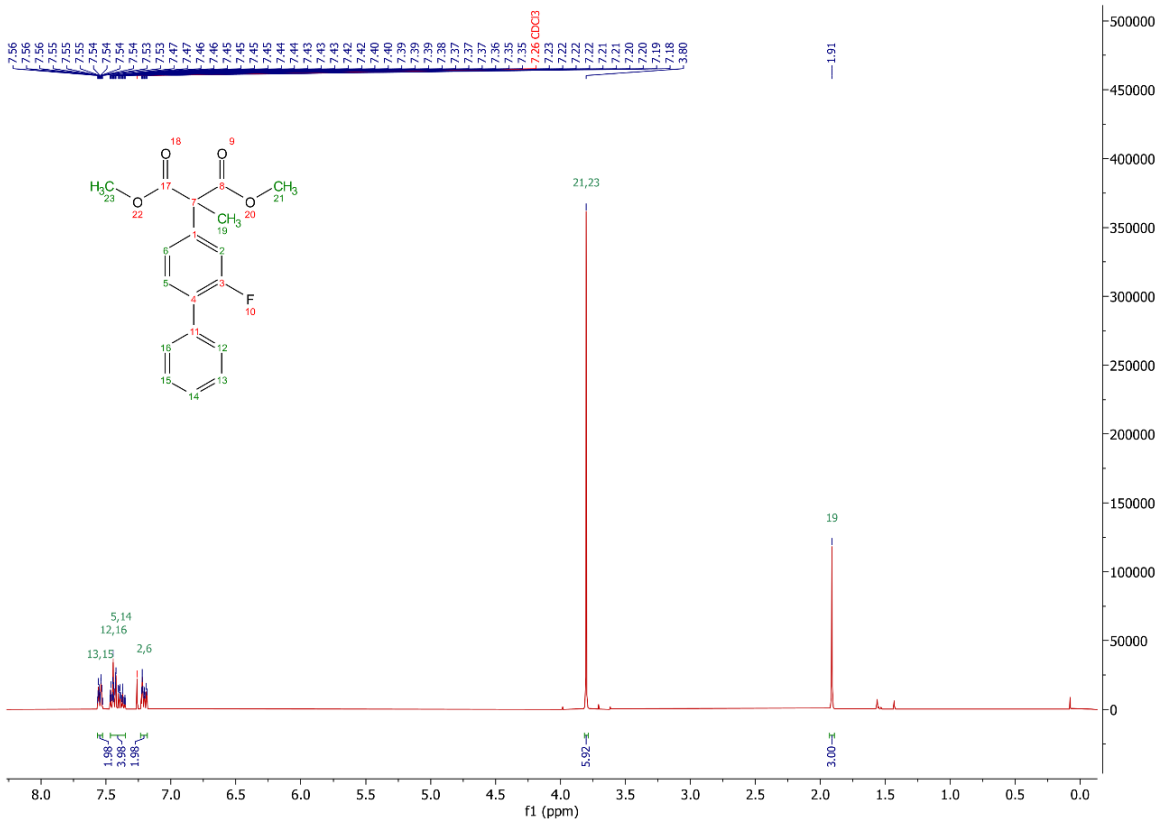

Figure S41. Measured ^{1}H-NMR spectrum of dimethyl 2-(2-fluoro-[1,1'-biphenyl]-4-yl)-2-methylmalonate (**2a**) in $CDCl_3$.

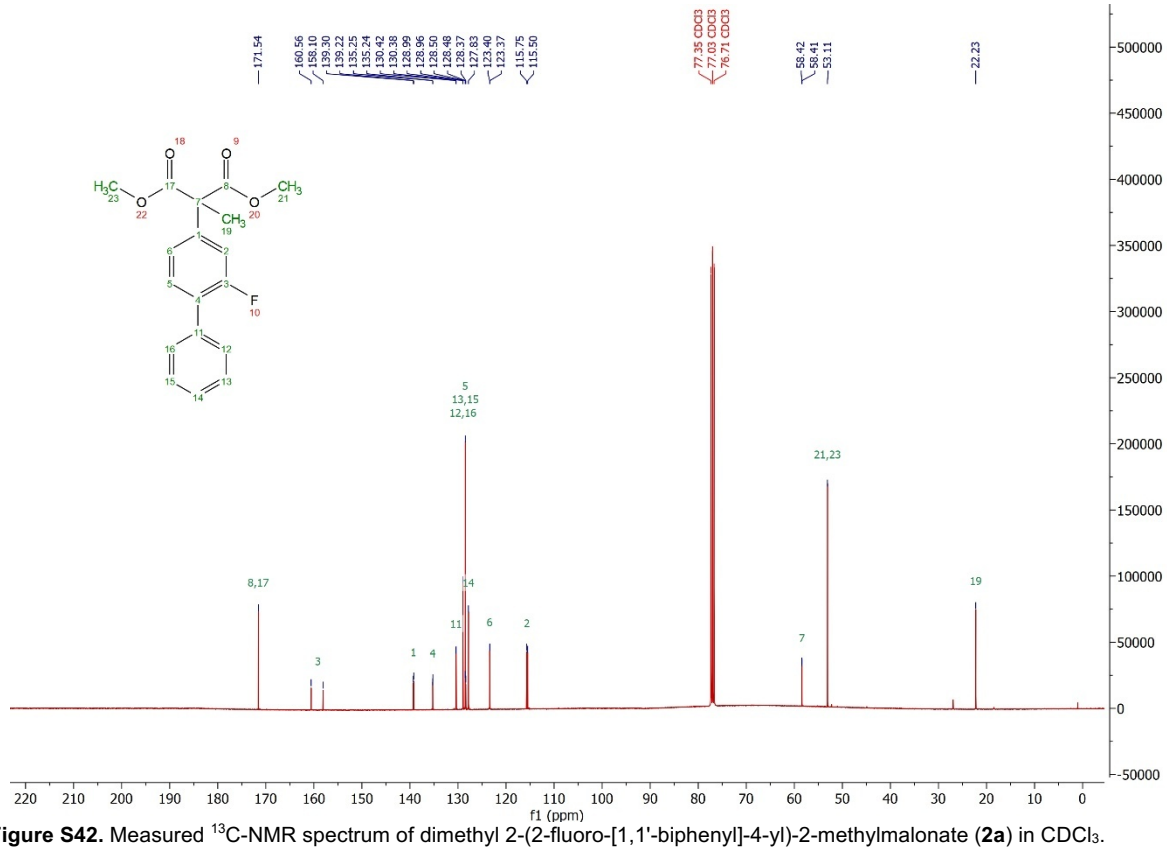

Figure S42. Measured ^{13}C-NMR spectrum of dimethyl 2-(2-fluoro-[1,1'-biphenyl]-4-yl)-2-methylmalonate (**2a**) in $CDCl_3$.

4.3 General Procedure for the Synthesis of 2-(6-methoxynaphthalen-2-yl)-2-methylmalonate (1b) and 2-(2-Fluoro-[1,1'-biphenyl]-4-yl)-2-methylmalonate (2b)

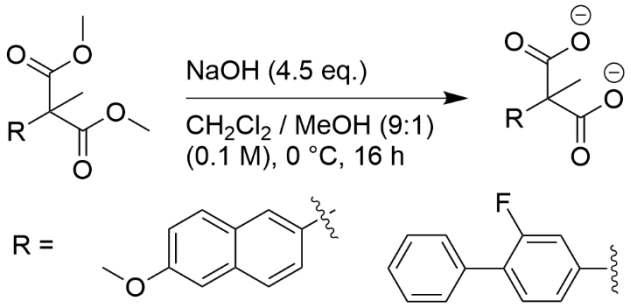

Dimethyl-naproxenmalonate (**1a**, 250.0 mg, 0.83 mmol, 1.0 eq.) or dimethyl-flurbiprofenmalonate (**2a**, 250.0 mg, 0.79 mmol, 1.0 eq.) was dissolved in CH_2Cl_2 / MeOH (9:1, 0.1 M, 7.9 mL). The solution was cooled to 0 °C and NaOH (4.5 eq.) was added against argon stream in one portion. The reaction mixture was stirred (600 rpm, 16 h) and allowed to warm to 22 °C. The reaction was cooled to 0 °C and diluted with double the volume of water. The organic solvents of the biphasic system were removed under reduced pressure to result the alkaline solution of sodium-naproxenmalonate or sodium-flurbiprofenmalonate, which were used without purification in the intensified process of enzymatic decarboxylation.

TLC: Cyclohexane:Ethylacetate, 1:5, 1% AcOH.

4.4 Synthesis of dimethyl phenylmalonate

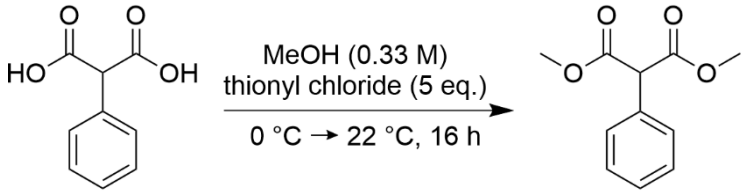

The synthesis of dimethyl phenylmalonate was carried out under inert atmosphere. Phenylmalonic acid (20.00 g, 111.0 mmol, 1.0 eq.) was dissolved in degassed methanol (333 mL, 0.33 M) and thionyl chloride (40.3 mL, 555.1 mmol, 5.0 eq.) was added dropwise while stirring (600 rpm) at 0 °C. The reaction mixture was allowed to warm to room temperature over 16 h. The reaction was terminated by the addition of a mixture of water and ice (100 mL) with adjustment to pH 4 with NaOH (10 M). The solvent was concentrated under reduced pressure, with subsequent extraction (EtOAc, 3 x 150 mL). The combined organic phases were washed with brine (200 mL) and dried over $MgSO_4$. The solvent was removed under reduced pressure. The white solid was recrystallized in methanol.

TLC: Cyclohexane:Ethylacetate, 1:5

Dimethyl phenylmalonate (19.29 g, 92.6 mmol, 83.5%).

^{1}H-NMR (400 MHz, $CDCl_3$): δ(ppm)= 7.43 – 7.31 (m, 5H), 4.65 (s, 1H), 3.76 (s, 6H).

^{13}C-NMR (101 MHz, $CDCl_3$): δ(ppm)= 168.70, 132.70, 129.37, 128.82, 128.48, 57.72, 53.00.

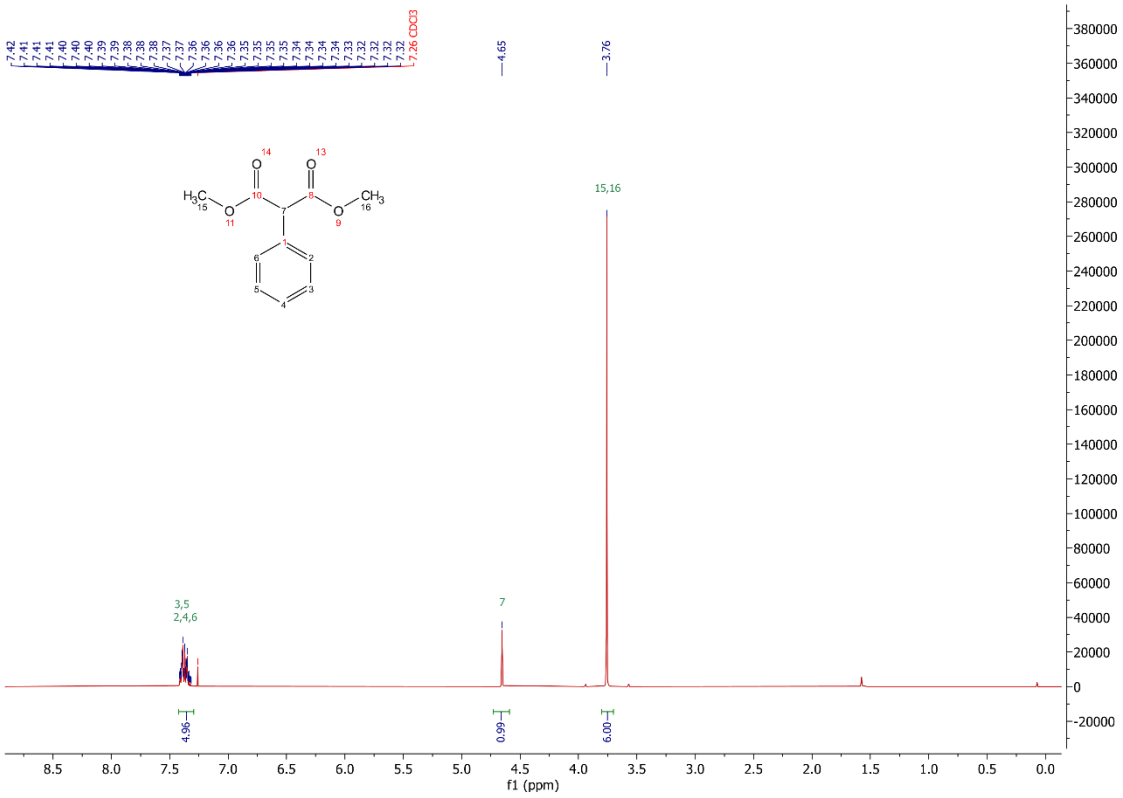

Figure S43. Measured ^{1}H-NMR spectrum of dimethyl phenylmalonate in $CDCl_3$.

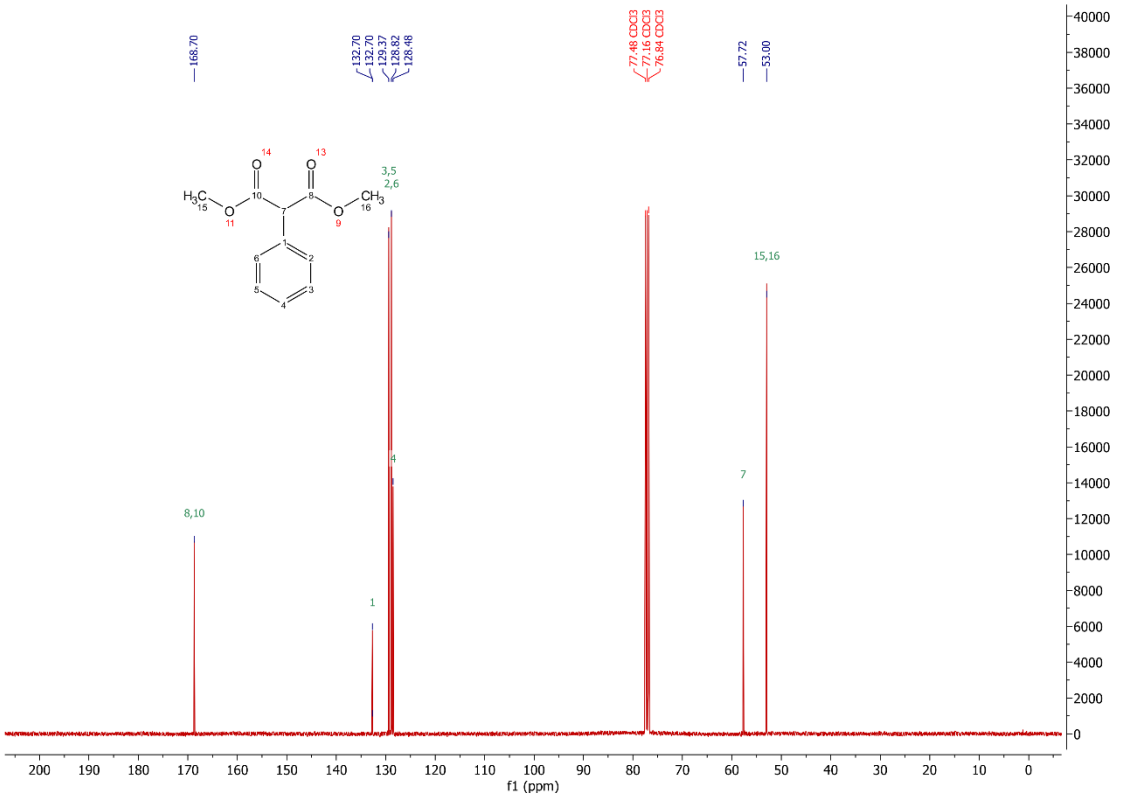

Figure S44. Measured ^{13}C-NMR spectrum of dimethyl phenylmalonate in $CDCl_3$.

4.5 Synthesis of dimethyl-2-methyl-2-phenylmalonate (3a)

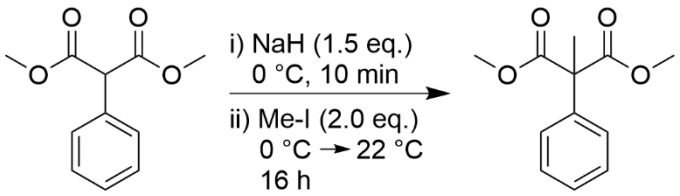

The synthesis of dimethyl-2-methyl-2-phenylmalonate was carried out under inert atmosphere. Sodium hydride (5.34 g, 134.1 mmol, 1.5 eq., 60% in mineral oil) was suspended in absolute dry DMF (0.2 M, total volume 463 mL) and dimethyl phenylmalonate (19.3 g, 92.6 mmol, 1.0 eq.) in DMF (63 mL) was added through a transfer cannula at 0 °C. The reaction mixture was stirred (600 rpm) for 10 minutes and methyl iodide (11.54 mL, 185.3 mmol, 2.0 eq.) was added dropwise over 15 min and the reaction mixture was allowed to warm to 22 °C overnight. The reaction was terminated with double the volume of water and ice and adjusted to pH 4 with HCl (5 M) and extracted with EtOAc (3 x 200 mL). The combined organic layers were washed brine (150 mL) and dried over $MgSO_4$. The crude was absorbed to diatomaceous earth and the solvent removed under reduced pressure. The absorbed crude was purified by dry column vacuum chromatography[77] to obtain a white solid.

TLC: Cyclohexane:Ethylacetate, 1:5.

Dimethyl-2-methyl-2-phenylmalonate (**3a**) (16.73 g, 75.3 mmol, 81.3%)

^{1}H-NMR (400 MHz, DMSO): δ(ppm)= 7.40 – 7.27 (m, 5H), 3.77 (s, 6H), 1.88 (s, 3H).

^{13}C-NMR (101 MHz, $CDCl_3$): δ(ppm)= 72.04, 138.20, 128.28, 127.71, 127.32, 58.88, 52.90, 22.41.

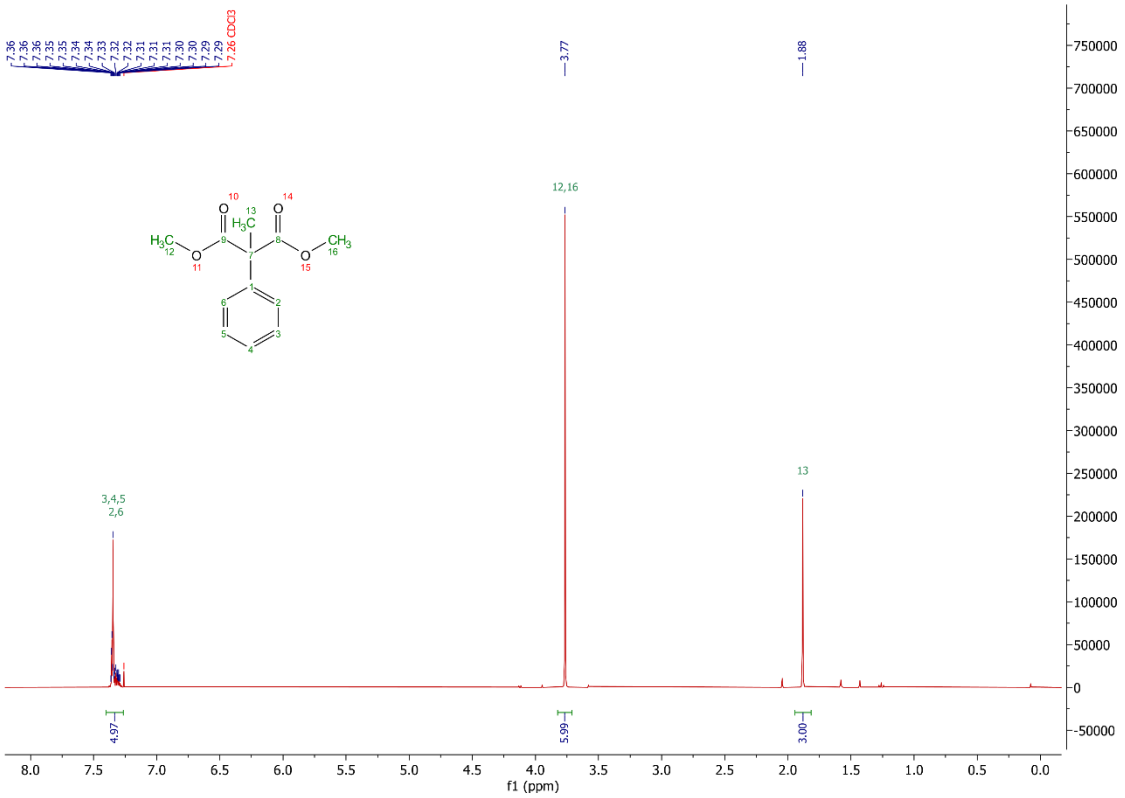

Figure S45. Measured ^{13}C-NMR spectrum of dimethyl-2-methyl-2-phenylmalonate (**3a**) in $CDCl_3$.

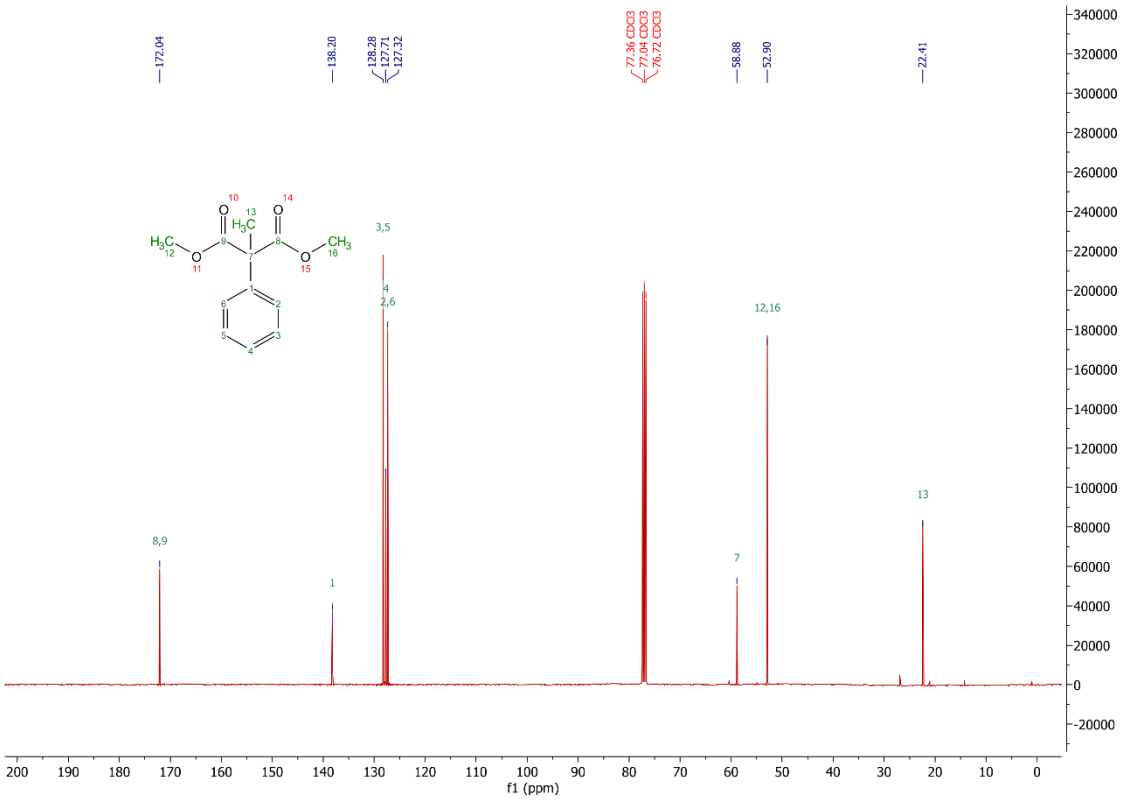

Figure S46. Measured ^{13}C-NMR spectrum of Dimethyl-2-methyl-2-phenylmalonate (**3a**) in $CDCl_3$.

4.6 Synthesis of 2-methyl-2-phenylmalonate

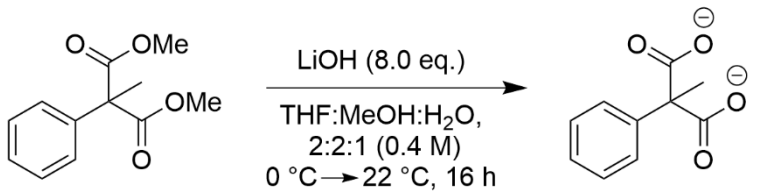

The synthesis of 2-alkyl-2-phenylmalonates was carried out under inert atmosphere. For this, dimethyl-2-alkyl-2-phenylmalonate (**3a**) (1.55 g, 8.0 mmol, 1.0 eq.) was dissolved in a solution of THF:MeOH:H_2O (2:2:1, 0.4 M, 20 mL) and degassed (5 min sparging argon, 1400 rpm). The solution was cooled to 0 °C and LiOH*H_2O (2.7 g, 63.8 mmol, 8.0 eq.) was added against argon stream in one portion. The reaction mixture was stirred (600 rpm) for 16 h. For the intensified biocatalytic process, 10 mL of water was added and the organic solvents were removed under reduced pressure from the reaction mixture. The resulted alkaline substrate solution was injected to the RBR without further steps.

4.7 Synthesis of 2-methyl-2-phenylmalonic acid

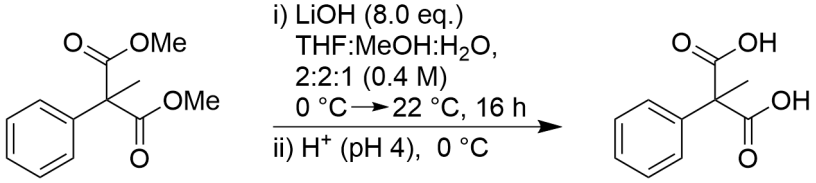

The synthesis of 2-methyl-2-phenylmalonate was carried out under inert atmosphere. For this, dimethyl-2-methyl-2-phenylmalonate (**3a**) (3.0 g, 13.5 mmol, 1.0 eq.) was dissolved in a solution of THF:MeOH:H_2O (2:2:1, 0.4 M, 63 mL) and degassed (5 min sparging argon, 1400 rpm). The solution was cooled to 0 °C and LiOH*H_2O (4.5 g, 109.0 mmol, 8.0 eq.) was added against argon stream in one portion. The reaction mixture was stirred (600 rpm) for 16 h.

For the isolation of 2-methyl-2-phenylmalonic acid the reaction mixture was diluted with double the volume of water and ice. Adjustment to pH 4 was done *carefully* with HCl (1 M) and extracted with EtOAc (3 x 100 mL). The combined organic layers were washed brine (50 mL) and dried over $MgSO_4$, followed by filtration through diatomaceous earth. The solvent was removed under reduced pressure to receive 2-alkyl-2-phenylmalonic acid without purification.

TLC: Cyclohexane:Ethylacetate, 1:5, 1% AcOH.

2-Methyl-2-phenylmalonic acid (**3b**) (2.54 g, 13.1 mmol, 96.3%)

^{1}H-NMR (400 MHz, DMSO): δ(ppm)= 7.40 – 7.30 (m, 4H), 7.32 – 7.22 (m, 1H), 1.71 (s, 3H).

^{13}C-NMR (400 MHz, DMSO): δ(ppm)= 172.90, 139.30, 127.85, 127.53, 127.05, 58.27, 22.28.

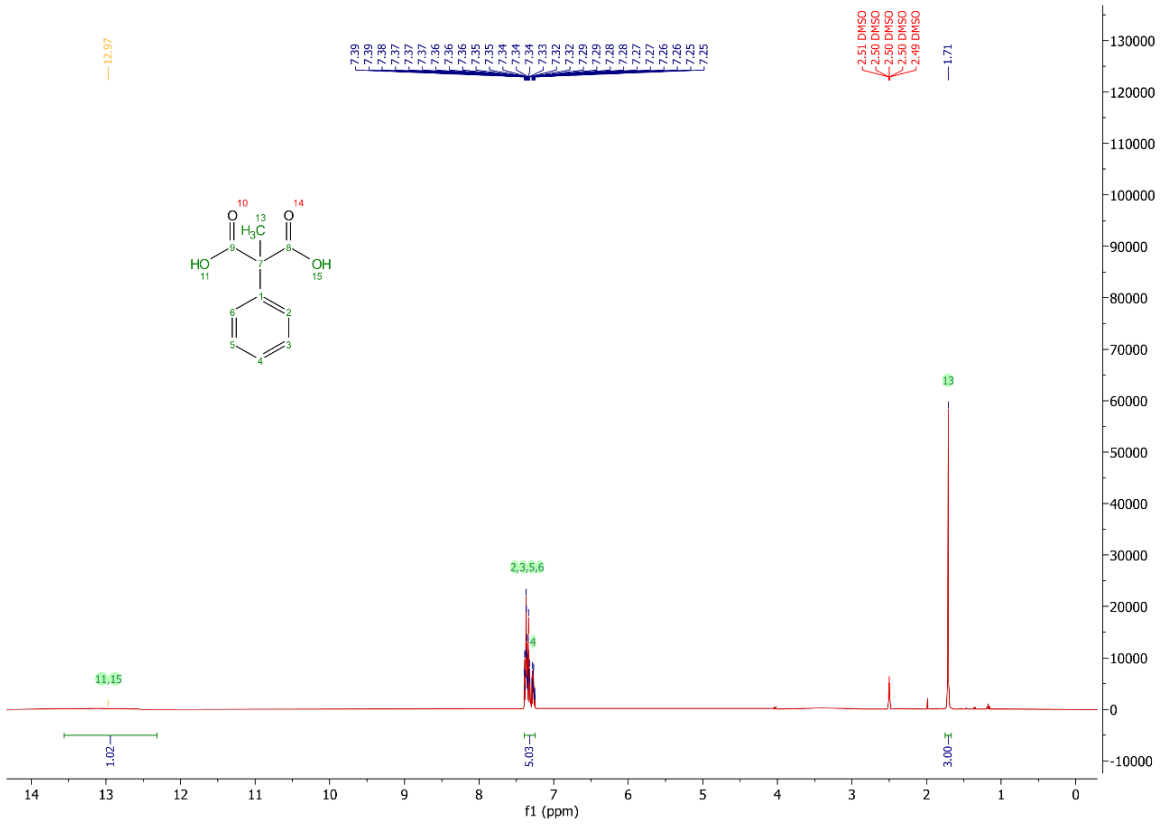

Figure S47. Measured ^{1}H-NMR spectrum of 2-methyl-2-phenylmalonate (**3b**) in DMSO-d6.

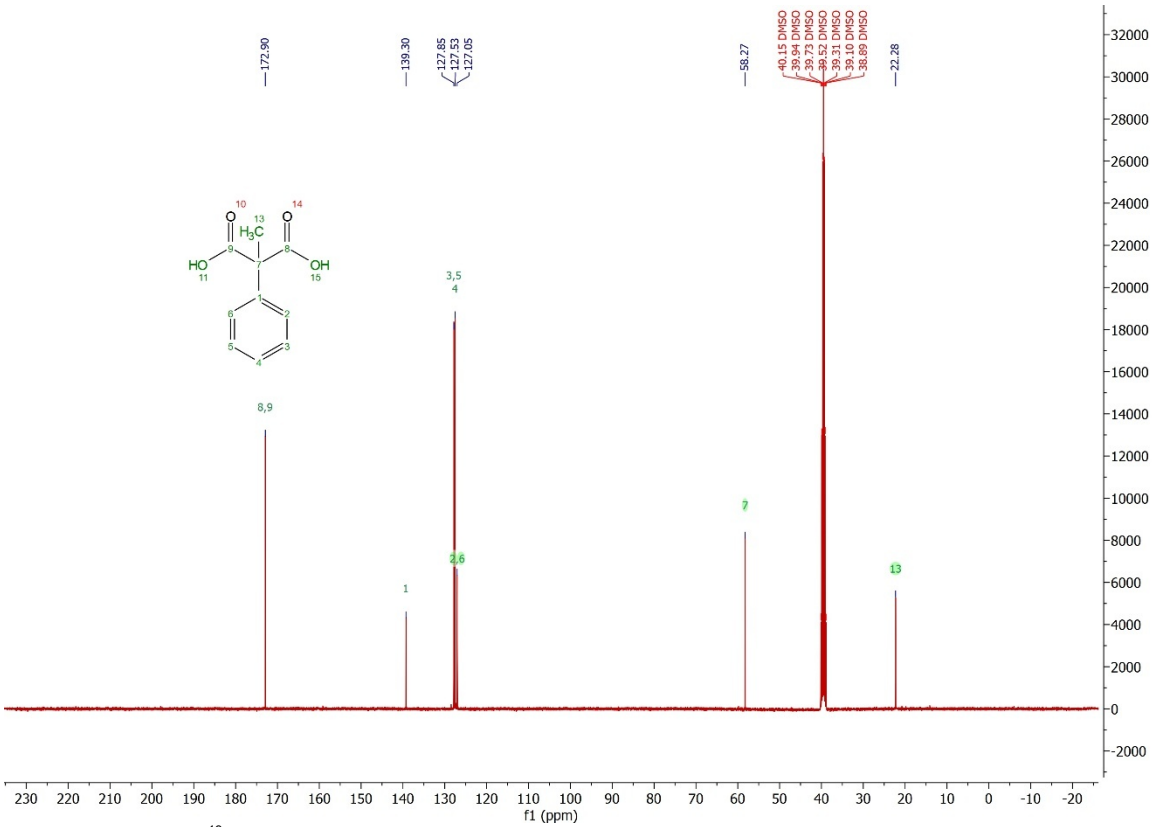

Figure S48. Measured ^{13}C-NMR spectrum of 2-methyl-2-phenylmalonate (**3b**) in DMSO-d6.

5. References

15 M. Aßmann, A. Stöbener, C. Mügge, S. K. Gaßmeyer, L. Hilterhaus, R. Kourist, A. Liese and S. Kara, *React. Chem. Eng.*, 2017, **2**, 531–540.

16 S. K. Gaßmeyer, J. Wetzig, C. Mügge and R. Kourist, *ChemCatChem*, 2016, **8**, 916–921.

28 J. Gerstenberger, T. Werbilo, R. Kourist and S. Kara, *ChemBioChem*, DOI:10.1002/cbic.70339.

36 E. van der Pol, J. Gerstenberger, X. Georgiadou, K. Schliep, C. Schür, S. Kara and R. Kourist, *bioRxiv*, 2026, 2026.01.14.699310.

50 T. A. Rogers and A. S. Bommarius, *Chem. Eng. Sci.*, 2010, **65**, 2118–2124.

60 P. Domínguez de María, ChemSusChem, 2025, **202501831**, 1–8.

65 C. E. Rasmussen and C. K. I. Williams, *Gaussian Processes for Machine Learning*, MIT press, Cambridge, 2006.

66 G. Derringer and R. Suich, *J. Qual. Technol.*, 1980, **12**, 214–219.

67 NIST/SEMATECH, Multiple responses: The desirability approach, https://www.itl.nist.gov/div898/handbook/pri/section5/pri5322.htm.

68 M. Siska, E. Pajak, K. Rosenthal, A. del Rio Chanona, E. von Lieres and L. M. Helleckes, Biotechnol. Bioeng., 2026, 1–32.

69 D. H. Ackley, A Connectionist Machine for Genetic Hillclimbing, Kluwer Academic Publishers, Boston, MA, 1987.

70 J. G. Proakis and D. G. Monolakis, Digital signal processing: principles, algorithms, and applications, Prentice-Hall, Inc., Upper Saddle River, New Jersey, Third Edit., 1996.

71 F. Hoffmeister and T. Bäck, in Parallel Problem Solving from Nature, eds. H.-P. Schwefel and R. Männer, Springer Berlin Heidelberg, Berlin, Heidelberg, 1991, pp. 455–469.

72 H. H. Rosenbrock, *Comput. J.*, 1960, **3**, 175–184.

73 E. Van Der Pol, T. Schlatzer, G. Hoffka, B. Di Geronimo, J. Eder, A. K. Schweiger, M. Karava, D. Gross, R. C. Fischer, D. Kracher, R. Kazlauskas, K. Miyamoto, S. Caroline, L. Kamerlin, R. Breinbauer and R. Kourist, *J. Am. Chem. Soc.*, 2025, **147**, 39271–39283.

74 E. Wiedenbeck, M. Kovermann, D. Gebauer and H. Cölfen, *Angew. Chemie - Int. Ed.*, 2019, **58**, 19103–19109.

75 S. Dohrn, C. Luebbert, K. Lehmkemper, S. O. Kyeremateng, M. Degenhardt and G. Sadowski, *Fluid Phase Equilib.*, 2021, **548**, 113200.

76 Y. Terao, Y. Ijima, H. Kakidani and H. Ohta, Bull. *Chem. Soc. Jpn.*, 2003, **76**, 2395–2397.

77 D. S. Pedersen and C. Rosenbohm, *Synthesis (Stuttg).*, 2001, 2431–2434.